Genomic plasticity drives olfactory adaptation in a pest fly

Qi Xue[1], Hany K. M. Dweck[1, *]

[1]Department of Entomology, The Connecticut Agricultural Experiment Station, New Haven, CT 06511, USA

*Corresponding author: hany.dweck@ct.gov

SUMMARY

Preference shifts in insects are often driven by changes in the olfactory system, yet the underlying mechanisms remain unclear. The worldwide pest *Drosophila suzukii*, which oviposits in ripe rather than overripe fruits, provides a powerful model to study these mechanisms and their behavioral consequences. Here, we show that this shift is linked to functional remodeling in four olfactory receptor neurons (ORNs): ab2B, ab3A, ab4B, and ab10A. While ab3A and ab10A exhibit tuning changes shared with the non-pest relative *D. biarmipes*, ab2B and ab4B display species-specific adaptations in *D. suzukii*. These changes result not only from receptor sequence divergence but also from novel innovations: receptor co-expression in ab3A and partitioned expression of Or67a paralogs in ab2B and ab10A. Together, these findings show how genomic plasticity in chemosensory gene families enables rapid sensory adaptation and niche transition.

INTRODUCTION

The olfactory system mediates the interactions between insects and their environment. It guides critical behaviors such as foraging, mate choice, and oviposition [1-4]. These behaviors are tightly linked to survival and reproductive success. This makes the olfactory system a key target of natural selection. The olfactory system, as a result, evolves rapidly in response to ecological shifts, particularly those involving changes in habitat, food resources, or reproductive sites [5-7]. However, the molecular mechanisms underlying olfactory adaptations remain poorly understood. While numerous studies have documented the remarkable variation in the copy number of chemosensory receptor genes, driven by gene gains and losses, across insect taxa[8-12], fewer have connected this genomic diversity to functional differences at the receptor and neuronal levels, or to shifts in behavior [6].

The worldwide fruit pest *D. suzukii* presents a powerful model to explore these evolutionary links. Unlike most *Drosophila* species, which are adapted to oviposit in fermenting fruit of no value, *D. suzukii* has evolved a distinct ecological niche [13,14]. It targets intact, ripening fruit for oviposition, causing significant agricultural losses[15]. This shift allows the species to exploit a previously underutilized resource, but it also poses new sensory and behavioral challenges. Navigating this niche requires the ability to detect and respond to a different set of volatile cues than those used by species that specialize on rotting substrates. Consequently, *D. suzukii*'s unique host preference is likely underpinned by extensive modifications to its olfactory system. Several molecular mechanisms are known to drive such adaptations, including amino acid substitutions that alter receptor tuning properties, changes in gene expression levels that modify receptor neuron sensitivity, and structural changes in the genome that increase or decrease receptor copy number through duplication, neofunctionalization, or pseudogenization [5,6,16-20].

Comparative genomic and transcriptomic analyses have revealed that *D. suzukii*'s odorant receptor (Or) repertoire exhibits distinctive evolutionary signatures [21-24]. Two gene expansions, *Or23a* and *Or67a*, set this species apart from its close relatives *D. biarmipes* and *D. melanogaster*. In *D. suzukii*, *Or23a* is present in four intact copies (*Or23a1*, *Or23a2*, *Or23a3*, and *Or23a4*), while *Or67a* is represented by four functional paralogs (*Or67a1*, *Or67a2*, *Or67a3*, and *Or67a4*) and one pseudogene (*Or67a5*). Interestingly, only the *Or67a* expansion is retained in *D. biarmipes* [22], suggesting that the expansion of *Or23a* occurred more recently in the *D. suzukii* lineage. In *D. melanogaster*, *Or23a* is expressed in the B neuron of antennal intermediate 2 (ai2) sensilla, but extensive functional screening has not identified strong ligands, leaving its role unresolved [25].

Or67a, by contrast, is better functionally characterized. In *D. melanogaster*, *Or67a* is expressed in the A neuron of ab10 sensilla, where it mediates strong responses to aromatic esters such as benzyl butyrate, benzyl acetate, and phenethyl propionate [25-27]. In *D. suzukii*, two copies of *Or67a* (*Or67a3* and *Or67a4*) exhibit signatures of positive selection [22], suggesting adaptive evolution potentially linked to the detection of odorants associated with ripening fruit.

Concurrently, *D. suzukii* has lost several ancestral Or genes, including *Or74a*, *Or85a*, and *Or98b* [22,23]. These losses could represent either relaxed selection for receptors tuned to volatiles no longer relevant in the new ecological context, or functional trade-offs associated with receptor repertoire remodeling.

Despite these striking genomic changes, the extent to which receptor gains and losses have reshaped the peripheral olfactory architecture, altering neuron identities, response properties, and overall coding capacity, remains largely unexplored.

Here, through a combination of electrophysiological recordings and comparative analyses, we identified olfactory receptor neurons whose response profiles differ markedly between *Drosophila suzukii* and its close relatives, *D. melanogaster* and *D. biarmipes*. Using molecular genetics, CRISPR/Cas9 gene editing, AlphaFold, and molecular docking, we elucidated the molecular mechanisms underlying these neuronal differences. Moreover, our work revealed that both gene losses and gains have shaped the olfactory repertoire of *D. suzukii*, driving its sensory adaptation and facilitating its ecological niche transition from fermenting to ripening fruits. These findings highlight how molecular changes at the receptor level translate into behavioral shifts that underpin the evolutionary success and pest status of *D. suzukii*.

RESULTS

Neurons whose responses differ between *D. suzukii* and *D. melanogaster*

To identify neurons that differ in their responses between *D. suzukii* and *D. melanogaster*, we compared odorant-evoked responses of olfactory receptor neurons (ORNs) in the antennal basiconic, intermediate, and trichoid sensilla of both species using single sensillum recordings (SSR). Modifications in the tuning of these neurons could result from gene births and deaths accompanying *D. suzukii*'s transition to ripe fruit and may underlie its novel specialization.

This analysis complements our prior work on maxillary palp basiconic and antennal coeloconic sensilla in *D. suzukii* [28,29] and together provides a comprehensive functional atlas of ORN responses across all sensillum types.

For this analysis, we used a panel of 113 ecologically relevant odorants, each tested at a 10^{-2} dilution, including acids, esters, alcohols, aldehydes, ketones, lactones, and terpenes. This analysis generated a dataset of 3,503 odorant–ORN combinations (Figure 1A) in each species (n = 3–6 per combination in *D. suzukii* and n = 3 per combination in *D. melanogaster*) and revealed that the odorant response profiles of most ORNs are qualitatively similar between the two species (Figure S1; Extended Data File S1 and S2). However, a subset of four ORNs displayed notable shifts in odorant tuning (Figure 1A). These ORNs are ab2B, ab3A, ab4B, and ab10A.

To validate and further dissect these interspecific differences, we performed a second round of SSR using an odorant panel that included the most potent ligands identified in our initial screen, together with ligands previously reported for the

corresponding ORNs. All odorants were tested at a 10^{-4} dilution to approximate naturalistic concentrations encountered by flies in the wild[30].

To differentiate between *D. suzukii*-specific changes and more broadly shared evolutionary trends, we included *D. biarmipes* in our analysis. This species is the closest extant relative of *D. suzukii* [31,32] and has no distinct preference for either overripe or ripe fruit [13,14,21].

To assess the robustness of these shifts within *D. suzukii*, we included two geographically distinct populations: the WT3 strain from California (*Dsuz-WT3*), which served as the reference genome strain [31], and an independent strain collected in North Carolina (*Dsuz*-NC).

Shared and species-specific shifts in *D. suzukii*

In ab3A neurons, we observed two kinds of changes, one of which is shared by *D. suzukii* and *D. biarmipes*. These included markedly reduced responses to volatiles that strongly activate this neuron in *D. melanogaster* (Figure 1B, D, E), including ethyl hexanoate, which is a fermentation product[33], and increased responses to an alternative set of esters, including isoamyl acetate and butyl acetate (Figure 1D), which are produced during fruit ripening[33].

The second kind of change is unique to *D. suzukii*. These included significantly stronger responses to isobutyl acetate, ethyl butyrate, and ethyl isovalerate compared to *D. biarmipes* and *D. melanogaster* (Figure 1D, F), as well as robust, dose-dependent responses to β-cyclocitral (Figure 1C, D, G), a volatile isoprenoid emitted by green foliage, including strawberry leaves[33]. By contrast, over a range of dilutions, this compound elicited little or no activity in the ab3A neurons of *D. biarmipes* and *D. melanogaster* (Figure 1C, D, G).

We also found intraspecific variation in responses to β-cyclocitral across *D. suzukii* strains. All ab3A neurons in the WT3 strain (California origin) responded robustly to β-cyclocitral, whereas responses in the North Carolina strain were more heterogeneous: some ab3A neurons responded strongly while others showed little or no response (Figure 1D).

In ab10A neurons, both *D. suzukii* and *D. biarmipes* exhibited reduced sensitivity to benzyl butyrate and benzyl acetate compared to *D. melanogaster* (Figure 1H,I) and enhanced responses to geranyl acetate, β-citronellol, isoamyl butyrate, 1-octen-3-ol, ethyl-3-hydroxyhexanoate, and diethyl succinate (Figure 1H,J,K).

In ab2B neurons, both *D. melanogaster* and *D. biarmipes* exhibited strong to ethyl 3-hydroxybutyrate, a compound closely associated with fermentation[34,35], whereas all three *D. suzukii* strains displayed strongly reduced sensitivity (Figure 2A, C, D). By contrast, ab2B neurons in *D. suzukii* responded robustly to a distinct set of esters, including isoamyl acetate, butyl acetate, pentyl acetate, benzyl acetate, and isoamyl

230 butyrate (Figure 2B,C,E,F). These esters are formed as part of the fruit ripening
231 process[33-35].
232
233 In ab4B neurons, all three species responded to veratrole, whereas all three *D.*
234 *suzukii* strains additionally responded to ethyl salicylate, methyl salicylate, methyl
235 benzoate, acetophenone, and 4-ethylguaiacol (Figure 2G–J).
236
237 Together, these findings reveal a mosaic of shared and species-specific olfactory
238 changes in *D. suzukii*. The shifts in ab3A and ab10A, shared with *D. biarmipes*, likely
239 reflect phylogenetic divergence, whereas the unique sensitivity of ab3A neurons to β-
240 cyclocitral and species-specific tuning in ab2B and ab4B neurons point to derived
241 adaptations supporting *D. suzukii*'s specialization on ripe fruit.
242
243 ***D. suzukii* ab3A neurons co-express two odorant receptors, one of which is**
244 **specifically tuned to β-cyclocitral**
245 We next focused on ab3A neurons, which display a robust response to the strawberry
246 leaf volatile β-cyclocitral. We hypothesized that this neuronal type in *D. suzukii* co-
247 expresses two receptors, one of which is specifically tuned to β-cyclocitral. This
248 hypothesis was based on three observations: (1) only *D. suzukii* ab3A neurons respond
249 robustly to β-cyclocitral, despite both *D. suzukii* and *D. biarmipes* having a single
250 functional gene (referred to as the *Or22a*-like receptor) at the locus that determines ab3A
251 responses in drosophilids, with 91% sequence identity between the two species; (2) the
252 North Carolina strain of *D. suzukii* harbors two ab3A populations, one responsive to β-
253 cyclocitral and one not; and (3) the chemical structure of β-cyclocitral, a cyclic isoprenoid
254 aldehyde, differs markedly from the long- and short-chain esters that typically activate
255 ab3A neurons in *D. suzukii* and other *Drosophila* species.
256
257 To test this hypothesis, we first expressed the *D. suzukii Or22a* (*DsuzOr22a*) in
258 the *D. melanogaster* ab3A "empty neuron" system [36], where the endogenous
259 *Or22a*/*Or22b* locus is deleted and replaced by *Gal4* (Figure 3A). Ectopic expression of
260 *DsuzOr22a* restored responses to a suite of esters that matched the tuning profile of
261 native *D. suzukii* ab3A neurons (Figure 3B, D). However, these neurons did not confer
262 responses to β-cyclocitral (Figure 3C, D), indicating that *DsuzOr22a* is not sufficient for
263 β-cyclocitral detection and that a second co-expressed receptor is required.
264
265 We next used CRISPR/Cas9-mediated mutagenesis to generate loss-of-function
266 alleles of *DsuzOr22a*. Two independent alleles were recovered: *DsuzOr22a*^{1}, carrying a
267 25-nt deletion, and *DsuzOr22a*^{2}, carrying a 4-nt deletion. Both mutations are predicted to
268 produce truncated, non-functional proteins of 106 amino acids (Figure 3E). To control for
269 potential background effects, we also generated heteroallelic *DsuzOr22a* mutant
270 combinations using these homozygous lines.
271
272 Compared to Wild-type, *DsuzOr22a*$^{1/+}$, and *DsuzOr22a*$^{2/+}$ flies, ab3A neurons in
273 *DsuzOr22a*^{1}*, DsuzOr22a*^{2}*, and DsuzOr22a*$^{1/}$*Or22a*^{2} mutant flies exhibited drastically
274 reduced responses to all tested esters (Figure 4F, H), demonstrating that *DsuzOr22a* is
275 required for ester sensitivity. However, responses to β-cyclocitral were intact in all

mutants, confirming that a second receptor mediates detection of this compound (Figure 4G, H).

To determine whether the β-cyclocitral receptor belongs to the odorant receptor (OR) or ionotropic receptor (IR) family, we measured responses from large basiconic sensilla in *D. suzukii Orco* mutant flies. Because *Orco* is an obligate co-receptor for all functional ORs but not IRs, the presence or absence of β-cyclocitral responses in this background would distinguish the receptor class.

We found that β-cyclocitral did not elicit any response in any of the 117 basiconic sensilla examined in *DsuzOrco* mutant flies, indicating that β-cyclocitral detection depends on *Orco* and thus is mediated by an OR rather than an IR (Figure S2).

Together, these results demonstrate that *D. suzukii* ab3A neurons co-express two odorant receptors: *Or22a*, which has shifted its tuning toward several ripening fruit esters such as isobutyl acetate, butyl acetate, and isoamyl acetate, and a second, as-yet-unidentified receptor that is specifically tuned to β-cyclocitral.

A Single Amino Acid Substitution Alters Ligand Specificity of *Or22a* in *D. suzukii*

We next investigated the molecular basis of the tuning shift of *DsuzOr22a*. We aligned the *Or22a* amino acid sequences from *D. melanogaster*, *D. suzukii*, and *D. biarmipes* using Clustal Omega and visualized the alignment with MView (Figure S3A). This analysis revealed 97 amino acid substitutions shared between *D. suzukii* and *D. biarmipes* relative to *D. melanogaster*, including a substitution at position 201 (aspartic acid [D] to alanine [A]). In *D. melanogaster* strains, the residue at this position is predicted to lie within the odorant-binding pocket[37], which is proposed to form within the extracellular leaflet of the plasma membrane between helices TM1–TM6[38]. Previous work showed variation at this site, together with changes at residue 92, alters ligand-binding specificity and contributes to phenotypic variation in ab3A responses among natural populations of *D. melanogaster*[38]. Since residue 92 is conserved across all three species, the substitution at position 201 likely plays a major role in the tuning shift of *DsuzOr22a*.

To determine the functional impact of this substitution, we used AlphaFold2 to model the wild-type *DsuzOr22a* (D201A) and an *in silico* variant with the A201D substitution. We then performed molecular docking with isobutyl acetate, a key ligand for *DsuzOr22a*. The predicted models revealed that the A201D substitution induces a pronounced reorganization of the binding pocket architecture, producing a conformation distinct from that of the wild-type receptor (Figure S3B). This suggests that D201A significantly alters receptor–ligand interactions and contribute to the tuning shift of *DsuzOr22a*.

We then tested this prediction by generating a site-directed mutant of *DsuzOr22a* (A201D) and expressing it in the *D. melanogaster* ab3A “empty neuron” system. This substitution did not increase the response of *DsuzOr22a* to any of the compounds that strongly activate *D. melanogaster* ab3A (Figure 3I,J). By contrast, it reduced responses to all tested odorants (Figure 3I,J). Interestingly, responses of the A201D variant to

isobutyl acetate across a range of dilutions more closely resembled that of *D. melanogaster* ab3A than of *D. suzukii* ab3A or wild-type *DsuzOr22a* (Figure 3J), indicating a partial reversion toward the ancestral tuning state. These results support a critical role for residue 201 in reshaping *Or22a* ligand specificity in *D. suzukii*, particularly for fruit-ripening esters.

Functional Analysis of *Or23a* and *Or67a* Paralogs in *D. suzukii*

Having demonstrated that the response to β-cyclocitral in *D. suzukii* ab3A depends on an odorant receptor other than Or22a and deciphered the molecular basis of the *DszuOr22a* tuning shift, we next investigated the contributions of the expanded Or23a (four paralogs) and Or67a (five paralogs) receptor subfamilies to β-cyclocitral sensitivity in ab3A neurons, as well as to tuning shifts in ab10A and ab2B neurons. To do this, we expressed each paralog individually in the *D. melanogaster* ab3A "empty neuron" system and measured odor-evoked responses across a broad panel of compounds.

We found that all *Or23a* paralogs showed little (<30 spikes/s) or no responses to any of the tested odorants (Extended Data File S3), indicating that their key ligands remain unidentified. Similarly, *Or67a5* did not respond to any odorant, consistent with its annotation as a pseudogene due to a premature stop codon (TAA) at nucleotide position 174 (Extended Data File S4).

By contrast, *Or67a1*, *Or67a2*, *Or67a3*, and *Or67a4* each exhibited robust and specific responses to multiple odorants (Figures 4). However, none of these receptors responded to β-cyclocitral with the same magnitude or sensitivity as the native ab3A neuron, indicating that the receptor mediating this response remains unidentified.

Co-expression of *Or67a1* and *Or67a2* Produces a Response Profile Closely Matching the Native ab10A Odor Response in *D. suzukii*

Or67a1 and *Or67a2* responded to an overlapping set of odorants, but differed in response magnitude for several compounds, including geranyl acetate, α-phellandrene, and β-citronellol (Figure 4A). The odorant response profile of *Or67a2* more closely resembled that of the native *D. suzukii* ab10A neurons than did *Or67a1* (Figure 4A), with a mean Euclidean distance of 116 ± 0.8 (SE) compared to 122 ± 1 for *Or67a1*.

To determine whether co-expression of both receptors is required to fully replicate the ab10A response profile, we expressed *Or67a1* and *Or67a2* together in the *D. melanogaster* ab3A "empty neuron" system. This co-expression produced responses that closely matched the ab10A response profile (Figure 4A), with a smaller Euclidean distance (107 ± 2.5) than either receptor alone. The simple interpretation of these results is that *Or67a1* and *Or67a2* are likely co-expressed in the *D. suzukii* ab10A neurons and that their combined activity produces the characteristic tuning of this neuronal type.

***Or67a4* is expressed in the ab2B neurons of *D. suzukii* and mediates their responses to odorants**

Or67a3 and *Or67a4*, on the other hand, displayed odorant response profiles that diverged markedly from that of ab10A neurons (Figure 4B). Surprisingly, the response profile of

368 each of *Or67a3* and *Or67a4* closely resembled that of the native *D. suzukii* ab2B neurons
369 (Figure 4B), with Or67a4 showing a smaller mean Euclidean distance (180 ± 2.5)
370 compared to Or67a3 (319 ± 2.7). However, co-expression of *Or67a3* and *Or67a4* in the
371 *D. melanogaster* ab3A "empty neuron" system produced a response profile more similar
372 to *Or67a3* (192 ± 1.4 SE, mean Euclidean distance) but distinct from that of each of the
373 native *D. suzukii* ab2B (229 ± 2.5) and *Or67a4* alone (218 ± 1.1) (Figure 4B). Taken
374 together, these results suggest that Or67a4 is the primary receptor expressed in ab2B
375 neurons and largely determines the response profile of this neuronal type.
376
377 To test this, we used CRISPR/Cas9 to generate an independent loss-of-function
378 allele of *DsuzOr67a*, carrying a 22-bp deletion (*DsuzOr67a4*^{1}) (Figure 5A). We also
379 established a heterozygous line from the homozygous mutant.
380
381 While wild-type and the heterozygous line responded indistinguishably, the ab2B
382 neurons in the *DsuzOr67a4*^{1} mutant allele exhibited extremely reduced responses to all
383 tested odorants (Figure 5B,C). These results suggest that *Or67a4* is expressed in *D.*
384 *suzukii* ab2B neurons and underlies their novel odorant response, which differs from that
385 of ab2B neurons in *D. melanogaster* and *D. biarmipes*.
386
387 Together, these findings reveal a clear functional and spatial partitioning among
388 the *Or67a* paralogs in *D. suzukii*. *Or67a1* and *Or67a2* are likely co-expressed in ab10A
389 neurons, while *Or67a4* is expressed in a separate neuronal type, ab2B. This partitioning
390 of expression suggests that gene duplication in the *Or67a* lineage has facilitated
391 subfunctionalization across distinct olfactory neuron types, enabling *D. suzukii* to broaden
392 its olfactory repertoire and fine-tune its detection of ecologically relevant odorants.
393
394 **DISCUSSION**
395 Our results reveal that the evolutionary shift in preference from overripe to ripe fruit in
396 *Drosophila suzukii,* a worldwide berry fly pest, is mirrored by functional changes in a
397 limited subset of ORNs. Specifically, four ORNs (ab2B, ab3A, ab4B, and ab10A) exhibit
398 altered odorant tuning in *D. suzukii* relative to *D. melanogaster*. Of these, ab3A and
399 ab10A exhibit shared tuning shifts in *D. suzukii* and its non-pest sibling species *D.*
400 *biarmipes*. These shared shifts likely reflect ancestral adaptations predating the
401 transition to ripe fruit use. By contrast, ab2B and ab4B show unique tuning profiles in *D.*
402 *suzukii*.
403
404 Importantly, these modifications are not solely the result of receptor sequence
405 evolution but are also mediated by innovative mechanisms, including the co-expression
406 of two distinct odorant receptors in a single ORN (as observed in ab3A) and the
407 partitioned expression of gene duplicates across different ORNs (as seen with the
408 *Or67a* paralogs in ab2B and ab10A). These strategies provide a flexible framework for
409 expanding olfactory function without requiring the evolution of entirely new neuronal
410 types, facilitating rapid and efficient sensory adaptation during ecological transitions.
411
412 **Receptor Co-expression Enables Novel Odor Tuning in ab3A of *D. suzukii***

The ab3A neurons of *D. suzukii* illustrate two distinct molecular innovations that align with its shift to ripe fruit. First, these neurons have lost responses to key fermentation volatiles that strongly activate ab3A in *D. melanogaster*. Instead, they have gained increased sensitivity to a new set of ripening-associated short-chain esters. Second, ab3A neurons in *D. suzukii* have acquired strong sensitivity to β-cyclocitral, a volatile isoprenoid commonly found in green plant tissues such as strawberry leaves[33]. This represents a major functional innovation, as neither *D. melanogaster* nor *D. biarmipes* ab3A neurons respond to this compound. Thus, detection of β-cyclocitral likely serves as a vegetative cue that signals the presence of a host plant bearing fruit, providing *D. suzukii* with a sensory advantage in locating oviposition sites while the fruit is still attached to the plant.

The capacity for functional plasticity in ab3A neurons is a recurring theme in *Drosophila* evolution. This neuronal type has repeatedly shifted its odorant tuning across species and even among populations, often in response to divergent ecological pressures[37,39-43]. These shifts are frequently mediated by amino acid changes in the *Or22* locus, which encodes the primary odorant receptor(s) in ab3A[20,41,43]. In the noni-specialist *D. sechellia*, for example, *Or22a* has acquired substitutions that enhance its sensitivity to methyl esters, which are abundant in noni fruit[41]. Genetic approaches have demonstrated that these sequence changes are sufficient to alter the ab3A sensitivity and that this receptor is important for mediating long-range attraction to noni[41].

Similarly, in *D. suzukii*, we identified multiple amino acid substitutions in *Or22a*, including two at known functional hotspots, I45A and D201A, previously implicated in tuning modulation in other *Drosophila* species[20,41]. Our structural modeling and molecular docking analyses indicate that the D201A substitution plays a key role in the tuning shift of *Or22a* in *D. suzukii*. This substitution reorganizes the architecture of the ligand-binding pocket, likely altering the shape and electrostatic environment of the odorant interface. Furthermore, functional assays using a site-directed A201D mutant revealed markedly reduced responses to odorants, with its responses to isobutyl acetate across dilutions more closely resembling those of *D. melanogaster* ab3A than *D. suzukii* ab3A or wild-type *DsuzOr22a*, indicating partial reversion to the ancestral tuning state. However, similar tuning shifts and a substitution at position 201 were also observed in *D. biarmipes*, suggesting that *Or22a* diversification occurred prior to the shift to ripe fruit and may have evolved under different selective pressures.

Despite the functional impact of *Or22a* sequence evolution, it alone cannot account for the novel β-cyclocitral sensitivity. This response is absent in both *D. melanogaster* and *D. biarmipes*, indicating that the gain of β-cyclocitral sensitivity is a derived feature unique to *D. suzukii*. Our genetic and functional analyses revealed that β-cyclocitral sensitivity is mediated by a second odorant receptor co-expressed with *Or22a* in ab3A neurons. The response to β-cyclocitral was eliminated in *Orco* mutant flies confirming that the receptor that mediates this response belongs to the OR family rather than the ionotropic or gustatory receptor families. Recruitment of a second receptor likely reflects the chemical dissimilarity of β-cyclocitral from typical *Or22a* ligands and represents a strategic expansion of the odorant space encoded by a single ORN. This co-expression may also enable more refined odorant coding: combined input from both receptors

459 indicates the presence of a high-quality oviposition site, while activation of *Or22a* alone
460 signals suboptimal substrates. Such combinatorial coding could sharpen host selection
461 and oviposition decisions.
462
463 ***Or67a* Gene Family Expansion and Deployment Across Neurons**
464 The ab10A and ab2B neurons in *D. suzukii* have also undergone substantial functional
465 and molecular remodeling. In *D. melanogaster*, ab10A neurons express a single receptor,
466 *Or67a*, tuned to a broad range of compounds[25,26], whereas ab2B neurons express *Or85a*,
467 which responds to esters and alcohols typically associated with microbial fruit
468 degradation[25-27,34].
469
470 The response profiles of these two neuronal types have shifted markedly during
471 *Drosophila* evolution[44-46]. Changes in ab10A are likely driven by *Or67a* gene expansion;
472 for example, *D. simulans* carries three *Or67a* paralogs, all expressed in ab10A and
473 contributing to its novel response profile[16]. By contrast, the mechanisms underlying ab2B
474 tuning shifts remain less well understood. In several species, changes in ab2B odorant
475 response profiles are associated with the loss of *Or85a*[44,45], but the receptors that replace
476 it remain unidentified.
477
478 In *D. suzukii*, *Or85a* is not detected in the genome[22,23], while *Or67a* has
479 expanded into five paralogs: four intact paralogs (*Or67a1* through *Or67a4*) and one
480 pseudogene, *Or67a5*, which contains a premature stop codon[22,23]. Our functional
481 characterization of these paralogs revealed a clear partitioning of activity. *Or67a1* and
482 *Or67a2* are likely co-expressed in ab10A neurons, and their co-expression produced a
483 response profile that is more similar to that of ab10A than either receptor alone. By
484 contrast, Or67a4 (and to a lesser extent Or67a3) exhibited responses that are similar to
485 those of ab2B neurons, and deletion of *Or67a4* severely reduced ab2B responses to
486 odorants, providing direct evidence that this receptor underlies the novel tuning of ab2B
487 neurons in *D. suzukii*.
488
489 *D. biarmipes* has also expanded *Or67a* into four functional paralogs. However,
490 only ab10A neurons show a tuning shift resembling that of *D. suzukii*, while ab2B
491 neurons retain a *D. melanogaster*-like odorant response profile, consistent with the
492 detection of *Or85a* in its genome.
493
494 These differences suggest that the recruitment of *Or67a4* (and most likely
495 *Or67a3*) into the ab2B neurons is a unique feature to *D. suzukii*, likely emerging after
496 the genomic loss of *Or85a*. As such, *D. biarmipes* represents an intermediate
497 evolutionary state: while it shows early signs of olfactory adaptation in ab3A and ab10A
498 neurons, it does not exhibit β-cyclocitral sensitivity in ab3A neurons, which in *D. suzukii*
499 arises from the co-expression of a second receptor alongside *Or22a*, nor does it show
500 evidence for receptor reassignment in ab2B.
501
502 In summary, by co-expressing a second OR with *Or22a* in ab3A and partitioning
503 *Or67a* paralogs between ab10A and ab2B, *D. suzukii* expands its odorant tuning
504 without creating new neuronal classes or rewiring central circuits. This illustrates how

505 gene loss, duplication, functional divergence, and receptor redeployment can reprogram
506 olfactory function to meet the demands of novel ecological niches.
507
508 **Limitations of the study**
509 A key limitation of our study is that, although we discovered that *D. suzukii* ab3A
510 neurons express an additional receptor enabling detection of β-cyclocitral, the identity of
511 this receptor remains unknown. Additionally, while our data indicate that *Or67a1* and
512 *Or67a2* are co-expressed in ab10A neurons and that *Or67a4* has replaced the ancestral
513 *Or85a* in ab2B neurons, *Or67a3* is also a strong candidate for ab2B expression, as its
514 ectopic expression produces responses resembling those of native ab2B neurons, and
515 no other ORN responses resemble those of Or67a3. Notably, *Or67a3* lies immediately
516 downstream of *Or67a4*, separated by fewer than 500 base pairs, raising the possibility
517 that our CRISPR-mediated knockout of *Or67a4* may have inadvertently affected *Or67a3*
518 expression. Finally, the regulatory mechanisms governing the partitioned expression of
519 *Or67a* paralogs across these distinct neurons in *D. suzukii* remain unresolved.
520
521 **Methods**
522 ***Drosophila* stocks**
523 Flies, 5-7 days old, were reared on corn syrup and soy four culture medium (Archon
524 Scientifc) at 24°C and 50% relative humidity in a 12:12-h light–dark cycle. *D.*
525 *melanogaster* Canton-S stock was CS-5. *D. suzukii* Connecticut (CT), North Carolina
526 (NC), and California genome (WT3) strains were obtained from Dr. Richard S. Cowles,
527 Dr. Maxwell J. Scott, and Dr. Joanna C. Chiu, respectively. *D. biarmipes* (14,023–
528 0361.04) stock was obtained from the Drosophila Species Stock Center. *D. suzukii*
529 *Orco*^{3} mutant line was obtained from Dr. Benjamin Prud'homme. The *D. melanogaster*
530 empty neuron system (*Or22ab*^{Gal4}) was obtained from Dr. John R. Carlson.
531
532 **Odorants**
533 Odorants of the highest available purity were obtained from Millipore Sigma, TCI
534 America, or Thermo Scientific Chemicals and stored as recommended. A complete list
535 of odorants is provided in Table S1. Odorants were dissolved in hexane (Millipore
536 Sigma, Catalog #139386). Odor presentation was performed by inserting a Pasteur
537 pipette tip into a hole in a 20 cm delivery tube, which directed a continuous airstream
538 over the labium. The airflow through the pipette was controlled using a Stimulus Air
539 Controller CS-55 V2 (Syntech), delivering a 0.5 s pulse. The wind speed at the position
540 of the mounted animal, after adding the odorized stimulus to the continuous airflow, was
541 approximately 50 cm s^{-1}. As an odor source, a cellulose filter disc (~1 cm diameter)
542 soaked with 10 µl of diluted odorant was placed inside a disposable borosilicate glass
543 Pasteur pipette (2 ml capacity, Fisher Scientific GSA). Odorants were presented
544 sequentially, with at least 60 s between presentations. For dose–response analyses,
545 odorants were delivered in increasing concentrations in logarithmic steps.
546
547 **Electrophysiology**
548 A single fly was placed in a 200-µL plastic pipette tip with its head directed towards the
549 narrower end to allow only the antennae to protrude. The pipette tip was then securely
550 attached to a glass microscope slide. The antenna was gently stabilized on a cover slip

using a glass capillary. The slide was then placed under a light microscope (BX51WI, Olympus, Tokyo, Japan) equipped with a 50 × objective (LMPLFLN 50X, Olympus) and 10 × eyepieces. A reference tungsten electrode (catalog no. 716000, A-M Systems), electrolytically sharpened to 1 μm tip diameter by dipping it repeatedly in a 10% KNO3 solution, was inserted into the eye. The recording tungsten electrode, identical to the reference electrode, was inserted gently into the base of a coeloconic sensillum. Signals were amplified (10 × ; Syntech Universal AC/DC Probe; http://www.syntech.nl), sampled (10,667 samples s^{-1}), and filtered (100–3000 Hz with 50/60 Hz suppression) via a USB-IDAC connection (Syntech) to a computer. Action potentials were extracted using Syntech AutoSpike 32 software. Responses as the increase (or decrease) in the action potential frequency (spikes/s) were calculated by subtracting the number of action potentials during the 0.5 s preceding the odor stimulation from the number of action potentials during the 0.5 s of odor stimulation. We then subtracted the response to hexane from the response to the odorant, and the differences are what we reported. The lifetime kurtosis (K) was calculated using the following formula described in [47].

Continuous airflow

A 20 cm glass tube with an inner diameter of approximately 4 mm supplied activated charcoal-filtered humidified air to the labium. Air, continuous and pulsed, was generated by a Stimulus Air Controller CS-55 V2 from Syntech (https://www.ockenfels-syntech.com/products/stimulus-controllers/). The end of the tube was placed about 1 cm from the preparation, and the continuous airflow near the mounted animal had a speed of approximately 40 cm s−1.

***Generating UAS-DsuzOr* lines**

Five *D. suzukii* WT3 females were collected, and whole animals were immediately homogenized for RNA extraction using TRIzol reagent (Invitrogen). The extracted RNA was treated with TURBO DNase (Invitrogen) to remove residual genomic DNA. 1 μg of purified RNA was used for cDNA synthesis with oligo(dT) primers using SuperScript IV Reverse Transcriptase (Invitrogen) for the generation of PCR template for subsequent amplifications of *DsuzOr* genes. PCR reactions were conducted using Phusion High-Fidelity DNA Polymerase (Thermo Scientific) under standard thermal cycling conditions in a Bio-Rad thermocycler. PCR products were separated on 1.0% agarose gel, and DNA fragments of the expected sizes were excised and purified according to the manufacturer's instructions (Wizard SV Gel and PCR Cleanup System, Promega).

DsuzOrs were cloned into the pJFRC81-10XUAS-IVS-Syn21-GFP-p10 vector (pJFRC81, Addgene plasmid #36432). Forward and reverse PCR primers of *DsuzOrs* were designed with 20 bp overhangs complementary to the regions flanking the GFP coding sequence in pJFRC81. The pJFRC81 vector was linearized by PCR using primers flanking the GFP sequence, with effective removal of the GFP coding region. Gibson assembly (NEB) was then used to ligate the amplified *DsuzOr* fragments into the linearized vector. The resulting constructs were transformed into bacteria and sequence-verified. Verified plasmids were injected into embryos of BDSC Stock #8622 by BestGene Inc. for PhiC31-mediated site-specific integration. Primers are provided in Table S2.

597
598
599 **CRISPR–Cas9-mediated genome engineering**
600 Single guide RNAs (sgRNAs) targeting *DsuzOrs* were designed using the online
601 CHOPCHOP tool (https://chopchop.cbu.uib.no/). sgRNAs were synthesized through *in*
602 *vitro* transcription using the GeneArt Precision gRNA Synthesis Kit (Thermo Fisher
603 Scientific). The sgRNA was mixed with Cas9 protein (TrueCut, Invitrogen) at a final
604 concentration of 200 ng/µl and 500ng/µl, respectively, in a 10 µl reaction with 1 µl of
605 injection buffer (300 mM sodium phosphate and 1 mM potassium chloride) and an
606 additional 1 µl of 2M potassium chloride. The sgRNA/Cas9 mixture was incubated at
607 37ºC for 10 min in a thermocycler to promote ribonucleoprotein (RNP) complex
608 formation. The resulting RNP solution was passed through a Millipore Ultrafree-MC filter
609 (0.45 µM pore size) and kept on ice until ready to use.
610
611 The microinjection of RNPs into *Drosophila* embryos was performed using a
612 FemtoJet 4i microinjector (Eppendorf). Injection needles were prepared from capillary
613 tubes (World Precision Instrument, 1B100F-4) using a micropipette puller (Model P-
614 1000, Sutter Instrument). One day before microinjection, approximately 300 flies (3-5
615 days old) were transferred to an egg-laying chamber (Flystuff Cat #59-100) containing a
616 Petri dish filled with 10 ml of egg-laying substrate composed of 25g agar and 200ml
617 molasses dissolved in 500 ml of water. To diminish the older eggs retained in the
618 females' ovaries, the egg-laying Petri dish was replaced every 20 min for at least 5
619 times before injection. Only embryos laid within 20 min were used for injection, and the
620 entire injection process was completed within 1h.
621
622 G0 females that emerged from injected embryos (G0) were crossed to wild-type
623 flies to generate G1 heterozygotes. G1 individuals with potential CRISPR-induced
624 mutations were crossed again to wild-type flies to produce G2 heterozygotes. G1 flies
625 were sacrificed for genotyping to confirm the mutation types. G2 heterozygotes were
626 self-crossed to obtain homozygous mutants and establish stable mutant lines. Mutants
627 were identified using a PCR-based screening strategy. Primers for sgRNA synthesis
628 and mutant screening are listed in Table S3.
629
630 **Structural prediction and molecular docking.**
631 The 3D homotetrameric structures of *DsuzOr22a*$^{WT(D201A)}$ and *DsuzOr22a*^{A201D} were
632 generated with AlphaFold2[48]. The highest-confidence predictions (*model_0*) were
633 selected for docking. The ligand, isobutyl acetate (SDF file), was obtained from
634 PubChem (https://pubchem.ncbi.nlm.nih.gov/) and converted to mol2 format with
635 OpenBabel (v3.1.1)[49]. Structural preparation of both the ligand and receptor subunits
636 was performed in PyMol (v3.1.4), and the resulting files were converted to PDBQT
637 format with AutoDockTools (v1.5.7). Molecular docking was carried out using AutoDock
638 Vina (v1.2.7) with a cubic grid box (20 Å x 20 Å x 20 Å) centered on the transmembrane
639 domains. Receptor–ligand interactions were analyzed with the Protein-Ligand
640 Interaction Profiler (v2.4.0) and visualized in PyMol (v3.1.4).
641
642

643 **Quantification and statistical analysis**
644 The heatmaps were generated in PAST. Euclidean distances were calculated in R
645 (version 4.2.3) using the 'moments' package, and other statistical tests were performed
646 in GraphPad Prism (version 10.0.1 [316]).
647
648 **Acknowledgements**
649 This work was supported by NIH grant K01 DC020145 to H.K.M.D.
650
651 **Contributions**
652
653 H.K.M.D. conceived the study. H.K.M.D. and Q.X. designed the experiments. H.K.M.D.
654 and Q.X. carried out the experiments. H.K.M.D. and Q.X. analysed the data. H.K.M.D.
655 and Q.X. prepared the original draft of the manuscript. H.K.M.D. and Q.X. read and
656 approved the final version of the manuscript.
657
658
659 **Figure legends**
660
661 **Figure 1. Shared shifts in odor tuning of ab3A and ab10A in *D. suzukii* and *D.***
662 ***biarmipes*.**
663
664 (A) Responses of ab2B, ab3A, ab4B, and ab10A neurons in *D. suzukii* (n = 3–6) and *D.*
665 *melanogaster* (n = 3) to the indicated odorants. Each odorant was tested at a 10^{-2}
666 dilution. Error bars indicate SEM.
667
668 (B) Example traces of the response of the ab3 sensillum type to a 10^{-4} dilution of ethyl
669 hexanoate in *D. suzukii* (CT-strain), *D. biarmipes*, and *D. melanogaster*.
670
671 (C) Example traces of the response of the ab3 sensillum type to a 10^{-4} dilution of β-
672 cyclocitral in *D. suzukii* (CT-strain), *D. biarmipes*, and *D. melanogaster*.
673
674 (D) Responses of ab3A in three strains of *D. suzukii*, *D. biarmipes*, and *D. melanogaster*
675 to a 10^{-4} dilution of each of the indicated odorants. One-way ANOVA followed by
676 Tukey's multiple comparison test; n = 10. Values marked with different letters are
677 significantly different. Error bars represent SEM.
678
679 (E-G) Responses of ab3A to different dilutions of ethyl hexanoate (E), isobutyl acetate
680 (F), and β-cyclocitral (G) in *D. suzukii* (CT-strain), *D. biarmipes*, and *D. melanogaster*.
681 One-way ANOVA followed by Tukey's multiple comparison test; n = 5 for each dilution.
682 Values indicated with different letters are significantly different. Error bars represent
683 SEM.
684
685 (H) Responses of ab10A in three strains of *D. suzukii*, *D. biarmipes*, and *D.*
686 *melanogaster* to a 10^{-4} dilution of each of the indicated odorants. One-way ANOVA
687 followed by Tukey's multiple comparison test; n = 10. Values indicated with different
688 letters are significantly different. Error bars represent SEM.

689
690 (I-K) Responses of ab3A to different dilutions of benzyl butyrate (I), β-citronellol (J), and
691 geranyl acetate (K) in *D. suzukii* (CT-strain), *D. biarmipes*, and *D. melanogaster*. One-
692 way ANOVA followed by Tukey's multiple comparison test; n = 5 for each dilution.
693 Values indicated with different letters are significantly different. Error bars represent
694 SEM.
695
696 **Figure 2. Species-specific shifts in odor tuning of ab2B and ab4B in *D. suzukii*.**
697
698 (A) Example traces of the response of the ab2 sensillum type to a 10^{-4} dilution of ethyl
699 3-hydroxybutyrate in *D. suzukii* (CT-strain), *D. biarmipes*, and *D. melanogaster*.
700
701 (B) Example traces of the response of the ab2 sensillum type to a 10^{-4} dilution of
702 isoamyl acetate in *D. suzukii* (CT-strain), *D. biarmipes*, and *D. melanogaster*.
703
704 (C) Responses of ab2B in three strains of *D. suzukii*, *D. biarmipes*, and *D. melanogaster*
705 to a 10^{-4} dilution of each of the indicated odorants. One-way ANOVA followed by
706 Tukey's multiple comparison test; n = 10. Values marked with different letters are
707 significantly different. Error bars represent SEM.
708
709 (D-F) Responses of ab2B to different dilutions of ethyl 3-hydroxybutyrate (D), isoamyl
710 acetate (E), and butyl acetate (F) in *D. suzukii* (CT-strain), *D. biarmipes*, and *D.*
711 *melanogaster*. One-way ANOVA followed by Tukey's multiple comparison test; n = 5 for
712 each dilution. Values indicated with different letters are significantly different. Error bars
713 represent SEM.
714
715 (G) Responses of ab4B in three strains of *D. suzukii*, *D. biarmipes*, and *D.*
716 *melanogaster* to 10^{-4} dilution of the indicated odorants. One-way ANOVA followed by
717 Tukey's multiple comparison test; n = 10. Values indicated with different letters are
718 significantly different. Error bars represent SEM.
719
720 (H-J) Responses of ab4B to different dilutions of ethyl salicylate (H), methyl salicylate
721 (I), and methyl benzoate (J) in *D. suzukii* (CT-strain), *D. biarmipes*, and *D.*
722 *melanogaster*. One-way ANOVA followed by Tukey's multiple comparison test; n = 5 for
723 each dilution. Values indicated with different letters are significantly different. Error bars
724 represent SEM.
725
726 **Figure 3. ab3A neurons in *D. suzukii* express two odorant receptors, one of which**
727 **is tuned to β-cyclocitral.**
728
729 (A) Illustration of the *D. melanogaster* empty neuron system.
730
731 (B) Example traces of the responses of *D. suzukii* ab3A neurons and *DsuzOr22a* to a
732 10^{-4} dilution of isobutyl acetate.
733 (C) Example traces of the responses of *D. suzukii* ab3A neurons and *DsuzOr22a* to a
734 10^{-4} dilution of β-cyclocitral.

735
736 (D) Responses of *D. suzukii* ab3A neurons and *DsuzOr22a* to eleven odorants, each
737 tested at a 10^{-4} dilution. ns=not significant; ****p<0.0001; Mann-Whitney test; n = 10.
738 Error bars represent SEM.
739
740 (E) Schematic illustrating the generation of DsuzOr22a mutants using CRISPR/Cas9-
741 mediated gene disruption.
742
743 (F) Example traces of the responses of ab3A neurons in wildtype *D. suzukii*,
744 *DsuzOr22a*^{1}, and *DsuzOr22a*^{2} to a 10^{-4} dilution of isobutyl acetate.
745
746 (F) Example traces of the responses of ab3A neurons in wildtype *D. suzukii*,
747 *DsuzOr22a*^{1}, and *DsuzOr22a*^{2} to a 10^{-4} dilution of β-cyclocitral.
748
749 (H) Responses of ab3A neurons in wildtype *D. suzukii*, *DsuzOr22a*$^{1/+}$, *DsuzOr22a*$^{2/+}$,
750 *DsuzOr22a*^{1}, and *DsuzOr22a*^{2} to a battery of eleven odorants, each tested at a 10^{-4}
751 dilution . One-way ANOVA followed by Tukey's multiple comparison test; n = 10. Values
752 indicated with different letters are significantly different. Error bars represent SEM.
753
754 (I) Responses of wildtype *D. suzukii* ab3A neurons, *DsuzOr22a*$^{WT(D201A)}$,
755 *DsuzOr22a*$^{(A201)}$, and wildtype *D. melanogaster* ab3A neurons to a battery of ten
756 odorants, each tested at a 10^{-4} dilution. One-way ANOVA followed by Tukey's multiple
757 comparison test; n = 10. Values indicated with different letters are significantly different.
758 Error bars represent SEM.
759
760 (I) Responses of wildtype *D. suzukii* ab3A neurons, *DsuzOr22a*$^{WT(D201A)}$,
761 *DsuzOr22a*$^{(A201)}$, and wildtype *D. melanogaster* ab3A neurons to different dilutions of
762 isobutyl acetate. One-way ANOVA followed by Tukey's multiple comparison test; n = 10.
763 Values indicated with different letters are significantly different. Error bars represent
764 SEM.
765
766 **Figure 4. Responses of *D. suzukii Or67a* paralogs to a battery of 119 odorants.**
767
768 (A) Responses of *DsuzOr67a1*, *DsuzOr67a2*, and *DsuzOr67a1+2* to a battery of 119,
769 each tested at a 10-4 dilution. n = 5. Error bars represent SEM.
770
771 (B) Responses of *DsuzOr67a3*, *DsuzOr67a4*, and *DsuzOr67a3+4* to a battery of 119,
772 each tested at a 10-4 dilution. n = 5. Error bars represent SEM.
773
774 **Figure 5. *Or67a4* is expressed in ab2B neurons.**
775
776 (A) Schematic illustrating the generation of the *DsuzOr67a4*^{1} mutant using
777 CRISPR/Cas9-mediated gene disruption.
778

779 (B) Example traces of the responses of ab2B neurons in wildtype *D. suzukii*,
780 *DsuzOr67a*$^{1/+}$, and *DsuzOr67a*^{1} to a 10^{-4} dilution of isoamyl acetate.
781
782 (C) Responses of ab2B neurons in wildtype *D. suzukii*, *DsuzOr67a*$^{1/+}$, and *DsuzOr67a*^{1}
783 to a panel of 15 odorants, each tested at a 10^{-4} dilution. One-way ANOVA followed by
784 Tukey's multiple comparison test; n = 10. Values indicated with different letters are
785 significantly different. Error bars represent SEM.
786
787
788 **Supplementary Tables and Figures**
789 **Table 1. List of odorants**
790

Odorants	**Source**	Catalog number
1-Heptanol	Millipore Sigma	72954
1-Nonanol	Millipore Sigma	74280
1-Octen-3-ol	Millipore Sigma	O5284
1-Propanol	Millipore Sigma	34871
2,3-Butanediol	Millipore Sigma	B84904
2-Methyl-1-butanol	Millipore Sigma	133051
2-Methyl-1-propanol	Millipore Sigma	538132
3-Methyl-1-butanol	Millipore Sigma	77664
2-Phenylethanol	Millipore Sigma	77861
6-Methyl-5-hepten-2-ol	Millipore Sigma	W488401
Ethanol	Millipore Sigma	459828
Farnesol	Millipore Sigma	43348
trans-2-Hexen-1-ol	Millipore Sigma	W256218
Butyraldehyde	Millipore Sigma	538191
Hexanal	Millipore Sigma	18109
Phenylacetaldehyde	Millipore Sigma	W287407
trans-2-Hexen-1-al	Millipore Sigma	132659
trans-2-nonenal	TCI America	N04835ML
trans,trans-2,4-nonadienal	TCI America	N05215ML
2,3-Butanedione	Millipore Sigma	11038
2-Acetoxy-3-butanone	Millipore Sigma	W352623
2-Heptanone	Millipore Sigma	537683
2-Nonanone	Millipore Sigma	W278505
3-Nonanone	Millipore Sigma	
3-Octanone	Millipore Sigma	136913
4-Methyl-3-hepten-2-one	Millipore Sigma	49722
Acetone	Millipore Sigma	90872
Acetophenone	Millipore Sigma	42163
2-Ethylhexanoic acid	Millipore Sigma	538701
2-Methylbutyric acid	Millipore Sigma	193070
2-Oxovaleric acid	Millipore Sigma	75950
3-Butenoic acid	Millipore Sigma	134716

Acetic acid	Millipore Sigma	A6283
Butyric acid	Millipore Sigma	B103500
Heptanoic acid	Millipore Sigma	W334804
Hexanoic acid	Millipore Sigma	153745
Isobutyric acid	Millipore Sigma	W222208
Linoleic acid	Millipore Sigma	62230
Myristic acid	Millipore Sigma	W276413
Octanoic acid	Millipore Sigma	C2875
Oleic acid	Millipore Sigma	O1008
Pentanoic acid	Millipore Sigma	75054
Propionic acid	Millipore Sigma	402907
trans-3-Hexenoic acid	Millipore Sigma	W317004
Benzyl acetate	Millipore Sigma	50475
Benzyl butyrate	Millipore Sigma	W214000
Butyl acetate	Millipore Sigma	W217417
Butyl butyrate	Millipore Sigma	W218618
Butyl hexanoate	Millipore Sigma	W220108
Butyl isovalerate	Millipore Sigma	W221805
cis-3-hexenyl acetate	Millipore Sigma	74597
cis-3-hexenyl butyrate	Millipore Sigma	W340210
cis-3-hexenyl lactate	Millipore Sigma	W369020
Citronellyl acetate	Millipore Sigma	W231118
Diethyl succinate	Millipore Sigma	W237701
Ethyl (methylthio)acetate	Millipore Sigma	W383503
Ethyl 3-(methylthio)propionate	Millipore Sigma	W334308
Ethyl 3-hydroxybutyrate	Thermo Scientific Chemicals	AC118540250
Ethyl 3-hydroxyhexanoate	Millipore Sigma	W354503
Ethyl acetate	Millipore Sigma	L000325ML
Ethyl benzoate	Millipore Sigma	W242217
Ethyl butyrate	Millipore Sigma	75563
Ethyl decanoate	Millipore Sigma	148970
Ethyl Heptanoate	Millipore Sigma	W243728
Ethyl hexanoate	Millipore Sigma	148962
Ethyl isovalerate	Millipore Sigma	71607
Ethyl lactate	TCI America	L000325ML
Ethyl octanoate	Millipore Sigma	W244910
Ethyl salicylate	Millipore Sigma	68291
Ethyl *trans*-2-butenoate	TCI America	C0418
Ethyl *trans*-2-octenoate	Millipore Sigma	W364304
Geranyl acetate	Millipore Sigma	173495
Hexyl-2-methylbutanoate	Millipore Sigma	W349909
Hexyl hexanoate	Millipore Sigma	W257206
Isoamyl acetate	Millipore Sigma	W205532
Isoamyl butyrate	Millipore Sigma	W206008
Isobutyl acetate	Thermo Scientific Chemicals	AAB2570009

Methyl benzoate	Millipore Sigma	18344
Methyl hexanoate	Millipore Sigma	259942
Methyl isobutyrate	Millipore Sigma	W269409
Methyl octanoate	Millipore Sigma	21719
Methyl salicylate	Millipore Sigma	76631
Pentyl acetate	Millipore Sigma	109584
Phenethyl propionate	Millipore Sigma	W286702
Phenyl acetate	Millipore Sigma	108723
trans-2-Hexenyl acetate	Millipore Sigma	W256404
α-Terpinyl acetate	Millipore Sigma	W304799
4-Ethylguaiacol	Millipore Sigma	39774
4-Methyl veratrole	Millipore Sigma	ALNH9A9DBBB4
Guaiacol	Millipore Sigma	W253200
Indole	TCI America	I002125G
p-Cresol	Millipore Sigma	42429
Veratrole	Millipore Sigma	W379905
Eugenol	Millipore Sigma	35995
Methyl Eugenol	Millipore Sigma	04607
1,4-Diaminobutane	Millipore Sigma	D13208
2-Phenylethylamine	Millipore Sigma	8073340005
Ammonia hydroxide	Millipore Sigma	338818
Cadaverine	Millipore Sigma	33211
Spermidine	Millipore Sigma	S2626
Pyridine	Millipore Sigma	27040
Pyrrolidine	Millipore Sigma	W352316
(+)-Limonene oxide	Millipore Sigma	218324
(R)-(+)-Limonene	Millipore Sigma	62118
(S)-(-)-Limonene	Millipore Sigma	62128
(-)-Menthone	Millipore Sigma	63677
(-)-*trans*-Caryophyllene	Millipore Sigma	75541
Farnesene	Millipore Sigma	W383902
Sabinene	Millipore Sigma	W530597
Terpinolene	Millipore Sigma	W304603
Valencene	Millipore Sigma	W344303
α-Ionone	Millipore Sigma	03642
α-Phellandrene	Millipore Sigma	W285611
α-Pinene	Millipore Sigma	147524
α-Terpineol	Millipore Sigma	04899
β-Citronellol	Millipore Sigma	C83201
β-Cyclocitral	Thermo Scientific Chemicals	AAB2570009
β-Ionone	Millipore Sigma	W259525
γ-Terpinene	Millipore Sigma	223190
γ-Decalactone	Millipore Sigma	93738
γ-Hexalactone	Millipore Sigma	68554
1-Heptadecene	Millipore Sigma	H1108

DEET	Millipore Sigma	36542
Diallyl disulfide	Millipore Sigma	30648

791
792
793 **Table 2. List of primers for UAS constructs**

	Forward primer (5' to 3')	Reverse primer (5' to 3')
DsuzOr22a	ATGTTAGCCAAATTTTTTCCGC	CTATTTAAACTTTTCGGCTAAG
DsuzOr23a-1	ATGAAACTCAGCAAGATTTCCG	TTATTTAAATGAAACTTGAGTTGGATG
DsuzOr23a-2	ATGAAACTCAGCAAGATCTTTG	TTACAAAAAAGAACCTTGGCCATC
DsuzOr23a-3	ATGGAACTCACCAAGATCCTTG	TTAAGTCCTCCGGTTTAGGGAG
DsuzOr23a-4	ATGGAACTCACCAAGATCCATG	TTATTTAAATGAAACTTGAGTTGGATG
DsuzOr23a-1+4	Or23a1 part: ATGAAACTCAGCAAGATTTCCG	Or23a1 part: tgttctttcactgactgagtttttgcagatggctggaaatgaaacttgagctggatggtc
	Or23a4 part: tcagtcagtgaaagaacaaaaccagacaggatggaactcaccaagatccttgagattgac	Or23a4 part: ttaaaatgaaactttagttggatg
DsuzOr67a-1	ATGATTGATTTAATAAAACAAAAAATTTTTG	TTACTTGTACATCATTCGAACGG
DsuzOr67a-2	ATGAGCATTGACTTAAAAAAGAAG	CTACTGATACATCATTCGAATGG
DsuzOr67a-3	ATGGCTATTAACTTGTTTAGAAAGG	TTACTGATACATTGTTCGAATGG
DsuzOr67a-4	ATGAGTGTCCAGTTTATCAAAAAAC	TTATTGACACACTGTTTTTATAGC
DsuzOr67a-5	ATGAGGGTCGACTCCTTGAAG	CTACTGATACATAGTTCGAAGAGC
Note: flanking regions were added to the forward (5'-CAACTTAAAAAAAAAAATCAAA-3') and reverse (5'-TAAAAACGATTCATTCTAGA-3') primers.		

794
795
796
797
798
799
800
801
802
803
804

805 **Table 3. Primers for CRISPR**

	Forward primer (5' to 3')	Reverse primer (5' to 3')
DsuzOr22a gRNA synthesize	TAATACGACTCACTATAGcactttcctctgaccaagca	TTCTAGCTCTAAAACtgcttggtcagaggaaagtg
DsuzOr22a screen	tgccaatatcgattgtcgtg	atactgaccgtgggacaaaca
DsuzOr67a4 gRNA synthesize	TAATACGACTCACTATAGATCGATGCCATACGTTGAGT	TTCTAGCTCTAAAACACTCAACGTATGGCATCGAT
DsuzOr67a4 screen	CGAGTCCTCGAAACCTGAAG	ATGCCGAACACCACGTTTAT

806
807
808
809 **Figure S1. Responses of ORNs housed in D. suzukii and *D. melanogaster***
810 **antennal Basiconic, and intermediate, and trichoid sensilla.**
811
812 (A,B) Heatmap of responses of ORNs housed in *D. suzukii* (A) and *D. melanogaster* (B)
813 antennal basiconic, intermediate, and trichoid sensilla to 113 odorants. Each odorant
814 was diluted in hexane and tested at a 10^{-2} dilution. Odorants are color coded by
815 functional group.
816
817 **Figure S2. Responses of large basiconic sensilla in *DsuzOrco*^{3} to β-cyclocitral.**
818
819 **Figure S3. A single amino acid substitution alters the architecture of the ligand-**
820 **binding pocket of Or22a in *D. suzukii*.**
821
822 (A) Alignment of *D. melanogaster*, *D. suzukii*, and *D. biarmipes Or22a* orthologs.
823
824 (B) the location of the ligand-binding pocket with docked isobutyl acetate.
825
826
827
828
829
830
831
832
833

References

1 Benton, R. *Drosophila* olfaction: past, present and future. *Proc Biol Sci* **289**, 20222054 (2022). https://doi.org:10.1098/rspb.2022.2054

2 Hansson, B. S. & Stensmyr, M. C. Evolution of insect olfaction. *Neuron* **72**, 698-711 (2011). https://doi.org:10.1016/j.neuron.2011.11.003

3 Joseph, R. M. & Carlson, J. R. *Drosophila* Chemoreceptors: A Molecular Interface Between the Chemical World and the Brain. *Trends Genet* **31**, 683-695 (2015). https://doi.org:10.1016/j.tig.2015.09.005

4 Montell, C. Drosophila sensory receptors-a set of molecular Swiss Army Knives. *Genetics* **217**, 1-34 (2021). https://doi.org:10.1093/genetics/iyaa011

5 Andersson, M. N., Löfstedt, C. & Newcomb, R. D. Insect olfaction and the evolution of receptor tuning. *Frontiers in Ecology and Evolution* **Volume 3 - 2015** (2015). https://doi.org:10.3389/fevo.2015.00053

6 Auer, T. O., Shahandeh, M. P. & Benton, R. *Drosophila sechellia*: A Genetic Model for Behavioral Evolution and Neuroecology. *Annu Rev Genet* **55**, 527-554 (2021). https://doi.org:10.1146/annurev-genet-071719-020719

7 Keesey, I. W. Sensory neuroecology and multimodal evolution across the genus Drosophila. *Frontiers in Ecology and Evolution* **Volume 10 - 2022** (2022). https://doi.org:10.3389/fevo.2022.932344

8 Nozawa, M. & Nei, M. Evolutionary dynamics of olfactory receptor genes in *Drosophila* species. *Proc Natl Acad Sci U S A* **104**, 7122-7127 (2007). https://doi.org:10.1073/pnas.0702133104

9 Peláez, J. N. *et al.* Evolution of chemosensory and detoxification gene families across herbivorous Drosophilidae. *G3 Genes|Genomes|Genetics* **13** (2023). https://doi.org:10.1093/g3journal/jkad133

10 Sánchez-Gracia, A., Vieira, F. G. & Rozas, J. Molecular evolution of the major chemosensory gene families in insects. *Heredity* **103**, 208-216 (2009). https://doi.org:10.1038/hdy.2009.55

11 Eyun, S. I. *et al.* Evolutionary history of chemosensory-related gene families across the Arthropoda. *Mol Biol Evol* **34**, 1838-1862 (2017). https://doi.org:10.1093/molbev/msx147

12 McBride, C. S., Arguello, J. R. & O'Meara, B. C. Five Drosophila genomes reveal nonneutral evolution and the signature of host specialization in the chemoreceptor superfamily. *Genetics* **177**, 1395-1416 (2007). https://doi.org:10.1534/genetics.107.078683

13 Dweck, H. K., Talross, G. J., Wang, W. & Carlson, J. R. Evolutionary shifts in taste coding in the fruit pest *Drosophila suzukii*. *Elife* **10** (2021). https://doi.org:10.7554/eLife.64317

14 Karageorgi, M. *et al.* Evolution of Multiple Sensory Systems Drives Novel Egg-Laying Behavior in the Fruit Pest *Drosophila suzukii*. *Curr Biol* **27**, 847-853 (2017). https://doi.org:10.1016/j.cub.2017.01.055

15 Yeh, D. A., Drummond, F. A., Gómez, M. I. & Fan, X. The economic impacts and management of spotted wing *Drosophila* (*Drosophila Suzukii*): The case of wild blueberries in Maine. *Journal of Economic Entomology* **113**, 1262-1269 (2020). https://doi.org:10.1093/jee/toz360

16 Auer, T. O., Álvarez-Ocaña, R., Cruchet, S., Benton, R. & Arguello, J. R. Copy number changes in co-expressed odorant receptor genes enable selection for sensory differences in *drosophilid* species. *Nat Ecol Evol* **6**, 1343-1353 (2022). https://doi.org:10.1038/s41559-022-01830-y

17 Goldman-Huertas, B. *et al.* Evolution of herbivory in *Drosophilidae* linked to loss of behaviors, antennal responses, odorant receptors, and ancestral diet. *Proc Natl Acad Sci U S A* **112**, 3026-3031 (2015). https://doi.org:10.1073/pnas.1424656112

882 18 Matsunaga, T. *et al.* Evolution of Olfactory Receptors Tuned to Mustard Oils in Herbivorous
883 Drosophilidae. *Mol Biol Evol* **39** (2022). https://doi.org:10.1093/molbev/msab362
884 19 Matsunaga, T. *et al.* Odorant receptors mediating avoidance of toxic mustard oils in
885 *Drosophila melanogaster* are expanded in herbivorous relatives. *bioRxiv* (2025).
886 https://doi.org:10.1101/2024.10.08.617316
887 20 Shaw, K. H., Johnson, T. K., Anderson, A., de Bruyne, M. & Warr, C. G. Molecular and
888 Functional Evolution at the Odorant Receptor Or22 Locus in *Drosophila melanogaster*.
889 *Molecular Biology and Evolution* **36**, 919-929 (2019).
890 https://doi.org:10.1093/molbev/msz018
891 21 Durkin, S. M. *et al.* Behavioral and Genomic Sensory Adaptations Underlying the Pest
892 Activity of *Drosophila suzukii*. *Mol Biol Evol* **38**, 2532-2546 (2021).
893 https://doi.org:10.1093/molbev/msab048
894 22 Hickner, P. V. *et al.* The making of a pest: Insights from the evolution of chemosensory
895 receptor families in a pestiferous and invasive fly, *Drosophila suzukii*. *BMC Genomics* **17**,
896 648 (2016). https://doi.org:10.1186/s12864-016-2983-9
897 23 Ramasamy, S. *et al.* The Evolution of olfactory gene families in *Drosophila* and the genomic
898 basis of chemical-Ecological adaptation in *Drosophila suzukii*. *Genome Biol Evol* **8**, 2297-
899 2311 (2016). https://doi.org:10.1093/gbe/evw160
900 24 Walker, W. B., 3rd *et al.* Comparative transcriptomic assessment of the chemosensory
901 receptor repertoire of *Drosophila suzukii* adult and larval olfactory organs. *Comp Biochem*
902 *Physiol Part D Genomics Proteomics* **45**, 101049 (2023).
903 https://doi.org:10.1016/j.cbd.2022.101049
904 25 Benton, R. *et al.* An integrated anatomical, functional and evolutionary view of the
905 *Drosophila* olfactory system. *EMBO reports* **0**, 1-22 (2025).
906 https://doi.org:https://doi.org/10.1038/s44319-025-00476-8
907 26 Dweck, H. K. M. *et al.* The Olfactory Logic behind Fruit Odor Preferences in Larval and Adult
908 *Drosophila*. *Cell Rep* **23**, 2524-2531 (2018). https://doi.org:10.1016/j.celrep.2018.04.085
909 27 Hallem, E. A. & Carlson, J. R. Coding of odors by a receptor repertoire. *Cell* **125**, 143-160
910 (2006). https://doi.org:10.1016/j.cell.2006.01.050
911 28 Dweck, H. K. *et al.* Olfactory channels associated with the *Drosophila* maxillary palp
912 mediate short- and long-range attraction. *Elife* **5** (2016).
913 https://doi.org:10.7554/eLife.14925
914 29 Xue, Q., Hasan, K. S., Dweck, O., Ebrahim, S. A. M. & Dweck, H. K. M. Functional
915 characterization and evolution of olfactory responses in coeloconic sensilla of the global
916 fruit pest *Drosophila suzukii*. *BMC Biol* **23**, 50 (2025). https://doi.org:10.1186/s12915-025-
917 02151-9
918 30 Depetris-Chauvin, A. *et al.* Evolution at multiple processing levels underlies odor-guided
919 behavior in the genus *Drosophila*. *Curr Biol* **33**, 4771-4785 e4777 (2023).
920 https://doi.org:10.1016/j.cub.2023.09.039
921 31 Chiu, J. C. *et al.* Genome of Drosophila suzukii, the spotted wing drosophila. *G3 (Bethesda)*
922 **3**, 2257-2271 (2013). https://doi.org:10.1534/g3.113.008185
923 32 Ometto, L. *et al.* Linking genomics and ecology to investigate the complex evolution of an
924 invasive *Drosophila* pest. *Genome Biol Evol* **5**, 745-757 (2013).
925 https://doi.org:10.1093/gbe/evt034
926 33 Keesey, I. W., Knaden, M. & Hansson, B. S. Olfactory specialization in *Drosophila suzukii*
927 supports an ecological shift in host preference from rotten to fresh fruit. *J Chem Ecol* **41**,
928 121-128 (2015). https://doi.org:10.1007/s10886-015-0544-3

34 Versace, E. *et al.* Physiological and behavioral responses in *Drosophila melanogaster* to odorants present at different plant maturation stages. *Physiol Behav* **163**, 322-331 (2016). https://doi.org:10.1016/j.physbeh.2016.05.027

35 Cha, D. H., Adams, T., Rogg, H. & Landolt, P. J. Identification and field evaluation of fermentation volatiles from wine and vinegar that mediate attraction of spotted wing *Drosophila, Drosophila suzukii*. *J Chem Ecol* **38**, 1419-1431 (2012). https://doi.org:10.1007/s10886-012-0196-5

36 Chahda, J. S. *et al.* The molecular and cellular basis of olfactory response to tsetse fly attractants. *PLoS Genet* **15**, e1008005 (2019). https://doi.org:10.1371/journal.pgen.1008005

37 Shaw, K. H., Johnson, T. K., Anderson, A., de Bruyne, M. & Warr, C. G. Molecular and Functional Evolution at the Odorant Receptor *Or22* Locus in *Drosophila melanogaster*. *Mol Biol Evol* **36**, 919-929 (2019). https://doi.org:10.1093/molbev/msz018

38 Butterwick, J. A. *et al.* Cryo-EM structure of the insect olfactory receptor Orco. *Nature* **560**, 447-452 (2018). https://doi.org:10.1038/s41586-018-0420-8

39 Dekker, T., Ibba, I., Siju, K. P., Stensmyr, M. C. & Hansson, B. S. Olfactory shifts parallel superspecialism for toxic fruit in *Drosophila melanogaster* sibling, *D. sechellia*. *Curr Biol* **16**, 101-109 (2006). https://doi.org:10.1016/j.cub.2005.11.075

40 Stensmyr, M. C., Dekker, T. & Hansson, B. S. Evolution of the olfactory code in the *Drosophila melanogaster* subgroup. *Proc Biol Sci* **270**, 2333-2340 (2003). https://doi.org:10.1098/rspb.2003.2512

41 Auer, T. O. *et al.* Olfactory receptor and circuit evolution promote host specialization. *Nature* **579**, 402-408 (2020). https://doi.org:10.1038/s41586-020-2073-7

42 Shaw, K. H. *et al.* Natural variation at the *Drosophila melanogaster Or22* odorant receptor locus is associated with changes in olfactory behaviour. *Open Biol* **11**, 210158 (2021). https://doi.org:10.1098/rsob.210158

43 Mansourian, S. *et al.* Wild African *Drosophila melanogaster* Are Seasonal Specialists on Marula Fruit. *Curr Biol* **28**, 3960-3968 e3963 (2018). https://doi.org:10.1016/j.cub.2018.10.033

44 Crowley-Gall, A. *et al.* Olfactory variation among closely related cactophilic *Drosophila* species. *J Comp Physiol A Neuroethol Sens Neural Behav Physiol* (2025). https://doi.org:10.1007/s00359-025-01744-7

45 de Bruyne, M., Smart, R., Zammit, E. & Warr, C. G. Functional and molecular evolution of olfactory neurons and receptors for aliphatic esters across the *Drosophila* genus. *J Comp Physiol A Neuroethol Sens Neural Behav Physiol* **196**, 97-109 (2010). https://doi.org:10.1007/s00359-009-0496-6

46 Keesey, I. W. *et al.* Functional olfactory evolution in *Drosophila* suzukii and the subgenus Sophophora. *iScience* **25**, 104212 (2022). https://doi.org:10.1016/j.isci.2022.104212

47 Silbering, A. F. *et al.* Complementary function and integrated wiring of the evolutionarily distinct *Drosophila* olfactory subsystems. *J Neurosci* **31**, 13357-13375 (2011). https://doi.org:10.1523/jneurosci.2360-11.2011

48 Jumper, J. *et al.* Highly accurate protein structure prediction with AlphaFold. *Nature* **596**, 583-589 (2021). https://doi.org:10.1038/s41586-021-03819-2

49 O'Boyle, N. M. *et al.* Open Babel: An open chemical toolbox. *J Cheminform* **3**, 33 (2011). https://doi.org:10.1186/1758-2946-3-33

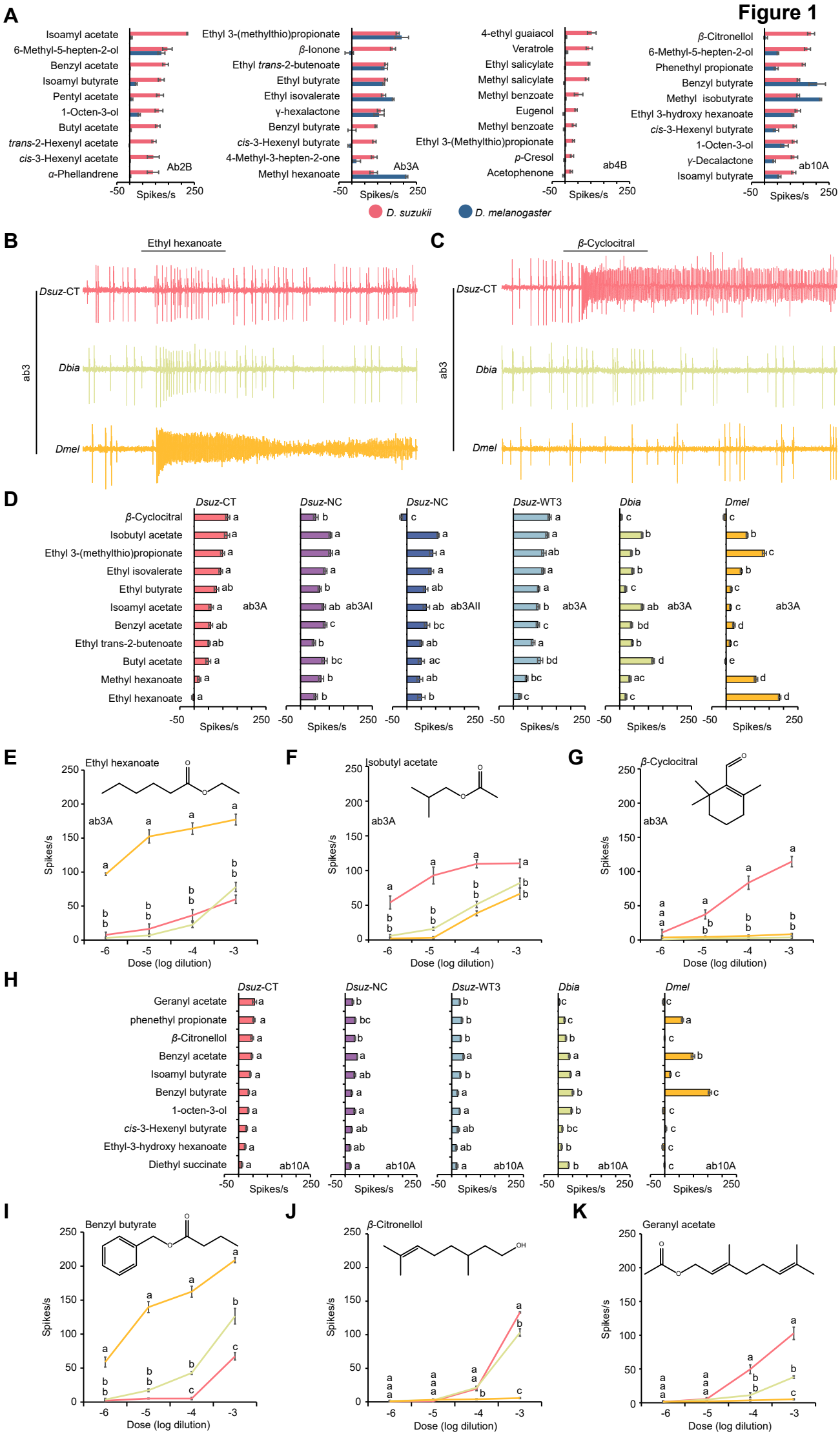
Figure 1
A
Isoamyl acetate
6-Methyl-5-hepten-2-ol
Benzyl acetate
Isoamyl butyrate
Pentyl acetate
1-Octen-3-ol
Butyl acetate
trans-2-Hexenyl acetate
cis-3-Hexenyl acetate
α-Phellandrene
Ab2B
Ethyl 3-(methylthio)propionate
β-Ionone
Ethyl trans-2-butenoate
Ethyl butyrate
Ethyl isovalerate
γ-hexalactone
Benzyl butyrate
cis-3-Hexenyl butyrate
4-Methyl-3-hepten-2-one
Methyl hexanoate
Ab3A
4-ethyl guaiacol
Veratrole
Ethyl salicylate
Methyl salicylate
Methyl benzoate
Eugenol
Methyl benzoate
Ethyl 3-(Methylthio)propionate
p-Cresol
Acetophenone
ab4B
β-Citronellol
6-Methyl-5-hepten-2-ol
Phenethyl propionate
Benzyl butyrate
Methyl isobutyrate
Ethyl 3-hydroxy hexanoate
cis-3-Hexenyl butyrate
1-Octen-3-ol
γ-Decalactone
Isoamyl butyrate
ab10A
-50
Spikes/s
250
D. suzukii
D. melanogaster
B
Ethyl hexanoate
Dsuz-CT
ab3
Dbia
Dmel
C
β-Cyclocitral
D
Dsuz-CT
Dsuz-NC
Dsuz-NC
Dsuz-WT3
Dbia
Dmel
β-Cyclocitral
Isobutyl acetate
Ethyl 3-(methylthio)propionate
Ethyl isovalerate
Ethyl butyrate
Isoamyl acetate
Benzyl acetate
Ethyl trans-2-butenoate
Butyl acetate
Methyl hexanoate
Ethyl hexanoate
ab3A
ab3AI
ab3AII
ab3A
ab3A
ab3A
E
Ethyl hexanoate
ab3A
Spikes/s
Dose (log dilution)
F
Isobutyl acetate
ab3A
G
β-Cyclocitral
ab3A
H
Dsuz-CT
Dsuz-NC
Dsuz-WT3
Dbia
Dmel
Geranyl acetate
phenethyl propionate
β-Citronellol
Benzyl acetate
Isoamyl butyrate
Benzyl butyrate
1-octen-3-ol
cis-3-Hexenyl butyrate
Ethyl-3-hydroxy hexanoate
Diethyl succinate
ab10A
I
Benzyl butyrate
J
β-Citronellol
K
Geranyl acetate

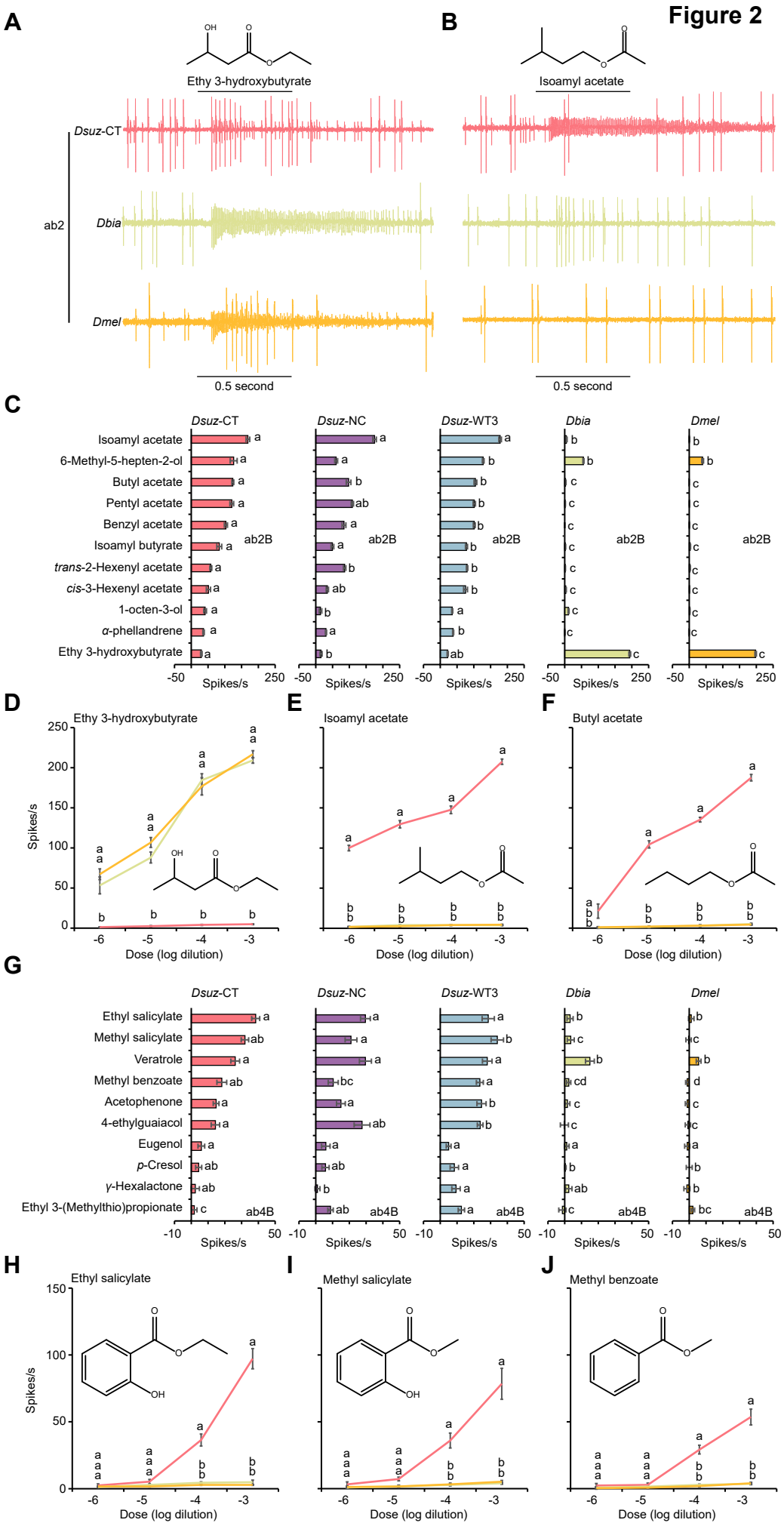
Figure 2
A
B
Ethy 3-hydroxybutyrate
Isoamyl acetate
Dsuz-CT
Dbia
Dmel
ab2
0.5 second
C
Dsuz-CT
Dsuz-NC
Dsuz-WT3
Dbia
Dmel
Isoamyl acetate
6-Methyl-5-hepten-2-ol
Butyl acetate
Pentyl acetate
Benzyl acetate
Isoamyl butyrate
trans-2-Hexenyl acetate
cis-3-Hexenyl acetate
1-octen-3-ol
α-phellandrene
Ethy 3-hydroxybutyrate
ab2B
Spikes/s
D
E
F
Ethy 3-hydroxybutyrate
Isoamyl acetate
Butyl acetate
Spikes/s
Dose (log dilution)
G
Ethyl salicylate
Methyl salicylate
Veratrole
Methyl benzoate
Acetophenone
4-ethylguaiacol
Eugenol
p-Cresol
γ-Hexalactone
Ethyl 3-(Methylthio)propionate
ab4B
Spikes/s
H
I
J
Ethyl salicylate
Methyl salicylate
Methyl benzoate
Spikes/s
Dose (log dilution)

Figure 3

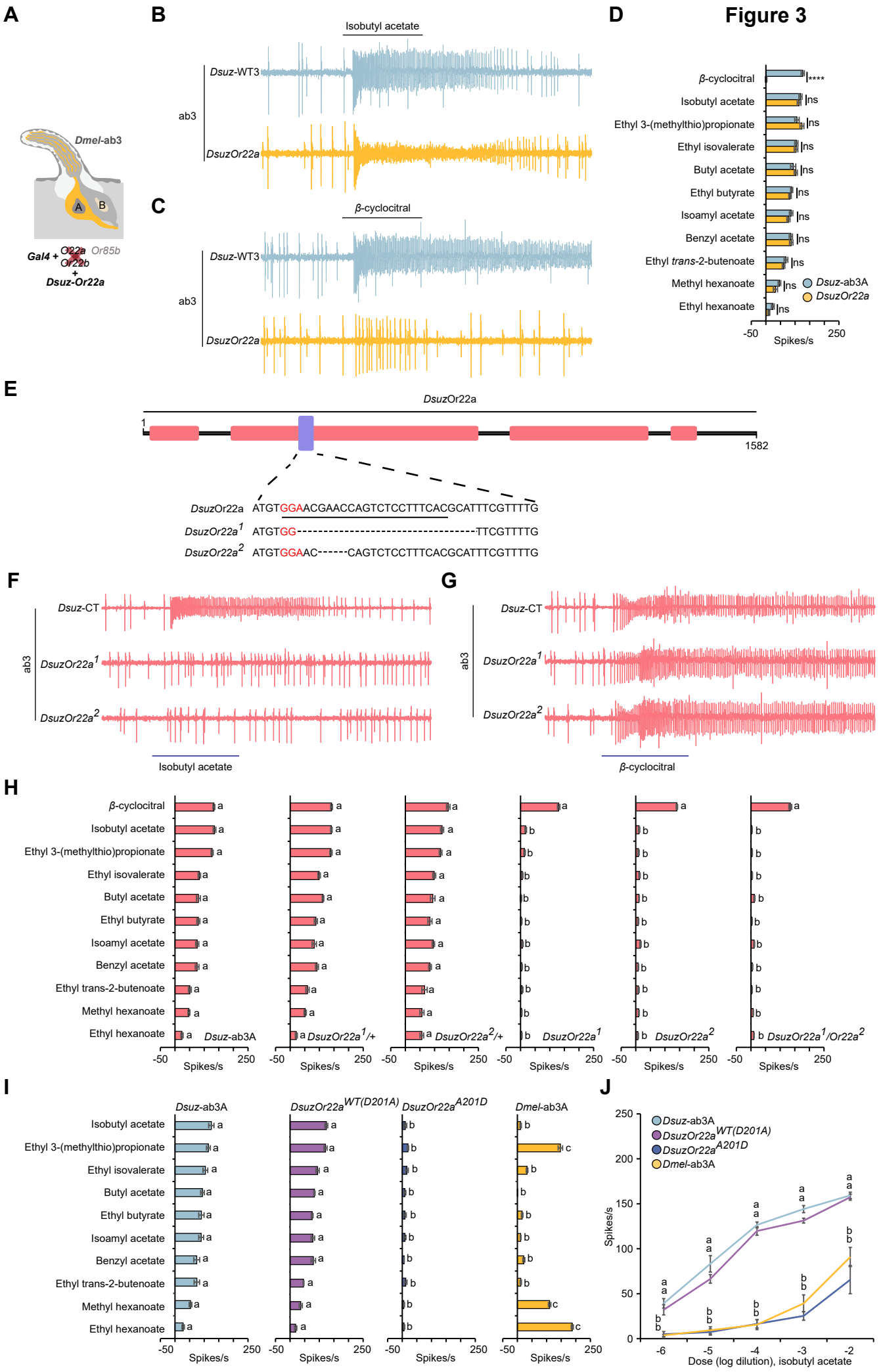
A
Dmel-ab3
A
B
Gal4 + Or22a Or85b
Or22b
+
Dsuz-Or22a
B
Isobutyl acetate
ab3
Dsuz-WT3
DsuzOr22a
C
β-cyclocitral
ab3
Dsuz-WT3
DsuzOr22a
D
β-cyclocitral
Isobutyl acetate
Ethyl 3-(methylthio)propionate
Ethyl isovalerate
Butyl acetate
Ethyl butyrate
Isoamyl acetate
Benzyl acetate
Ethyl trans-2-butenoate
Methyl hexanoate
Ethyl hexanoate
****
ns
Dsuz-ab3A
DsuzOr22a
-50
Spikes/s
250
E
DsuzOr22a
1
1582
DsuzOr22a ATGTGGAACGAACCAGTCTCCTTTCACGCATTTCGTTTTG
DsuzOr22a1 ATGTGG----------TTCGTTTTG
DsuzOr22a2 ATGTGGAAC------CAGTCTCCTTTCACGCATTTCGTTTTG
F
ab3
Dsuz-CT
DsuzOr22a1
DsuzOr22a2
Isobutyl acetate
G
ab3
Dsuz-CT
DsuzOr22a1
DsuzOr22a2
β-cyclocitral
H
β-cyclocitral
Isobutyl acetate
Ethyl 3-(methylthio)propionate
Ethyl isovalerate
Butyl acetate
Ethyl butyrate
Isoamyl acetate
Benzyl acetate
Ethyl trans-2-butenoate
Methyl hexanoate
Ethyl hexanoate
Dsuz-ab3A
DsuzOr22a1/+
DsuzOr22a2/+
DsuzOr22a1
DsuzOr22a2
DsuzOr22a1/Or22a2
-50
Spikes/s
250
I
Dsuz-ab3A
DsuzOr22aWT(D201A)
DsuzOr22aA201D
Dmel-ab3A
Isobutyl acetate
Ethyl 3-(methylthio)propionate
Ethyl isovalerate
Butyl acetate
Ethyl butyrate
Isoamyl acetate
Benzyl acetate
Ethyl trans-2-butenoate
Methyl hexanoate
Ethyl hexanoate
-50
Spikes/s
250
J
Dsuz-ab3A
DsuzOr22aWT(D201A)
DsuzOr22aA201D
Dmel-ab3A
Spikes/s
250
200
150
100
50
0
-6
-5
-4
-3
-2
Dose (log dilution), isobutyl acetate

Figure 4

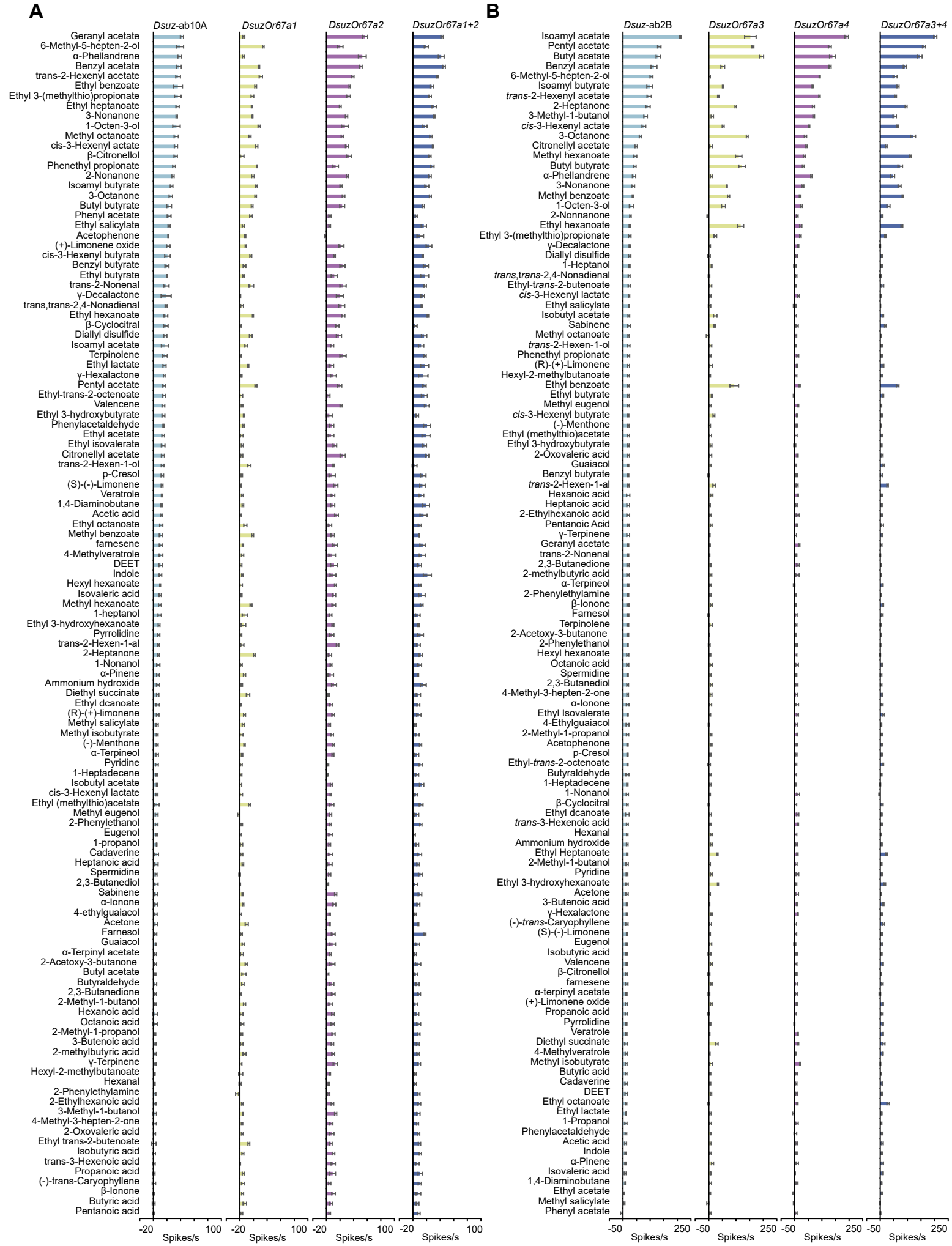
A
Dsuz-ab10A
DsuzOr67a1
DsuzOr67a2
DsuzOr67a1+2
Geranyl acetate
6-Methyl-5-hepten-2-ol
α-Phellandrene
Benzyl acetate
trans-2-Hexenyl acetate
Ethyl benzoate
Ethyl 3-(methylthio)propionate
Ethyl heptanoate
3-Nonanone
1-Octen-3-ol
Methyl octanoate
cis-3-Hexenyl actate
β-Citronellol
Phenethyl propionate
2-Nonanone
Isoamyl butyrate
3-Octanone
Butyl butyrate
Phenyl acetate
Ethyl salicylate
Acetophenone
(+)-Limonene oxide
cis-3-Hexenyl butyrate
Benzyl butyrate
Ethyl butyrate
trans-2-Nonenal
γ-Decalactone
trans,trans-2,4-Nonadienal
Ethyl hexanoate
β-Cyclocitral
Diallyl disulfide
Isoamyl acetate
Terpinolene
Ethyl lactate
γ-Hexalactone
Pentyl acetate
Ethyl-trans-2-octenoate
Valencene
Ethyl 3-hydroxybutyrate
Phenylacetaldehyde
Ethyl acetate
Ethyl isovalerate
Citronellyl acetate
trans-2-Hexen-1-ol
p-Cresol
(S)-(-)-Limonene
Veratrole
1,4-Diaminobutane
Acetic acid
Ethyl octanoate
Methyl benzoate
farnesene
4-Methylveratrole
DEET
Indole
Hexyl hexanoate
Isovaleric acid
Methyl hexanoate
1-heptanol
Ethyl 3-hydroxyhexanoate
Pyrrolidine
trans-2-Hexen-1-al
2-Heptanone
1-Nonanol
α-Pinene
Ammonium hydroxide
Diethyl succinate
Ethyl dcanoate
(R)-(+)-limonene
Methyl salicylate
Methyl isobutyrate
(-)-Menthone
α-Terpineol
Pyridine
1-Heptadecene
Isobutyl acetate
cis-3-Hexenyl lactate
Ethyl (methylthio)acetate
Methyl eugenol
2-Phenylethanol
Eugenol
1-propanol
Cadaverine
Heptanoic acid
Spermidine
2,3-Butanediol
Sabinene
α-Ionone
4-ethylguaiacol
Acetone
Farnesol
Guaiacol
α-Terpinyl acetate
2-Acetoxy-3-butanone
Butyl acetate
Butyraldehyde
2,3-Butanedione
2-Methyl-1-butanol
Hexanoic acid
Octanoic acid
2-Methyl-1-propanol
3-Butenoic acid
2-methylbutyric acid
γ-Terpinene
Hexyl-2-methylbutanoate
Hexanal
2-Phenylethylamine
2-Ethylhexanoic acid
3-Methyl-1-butanol
4-Methyl-3-hepten-2-one
2-Oxovaleric acid
Ethyl trans-2-butenoate
Isobutyric acid
trans-3-Hexenoic acid
Propanoic acid
(-)-trans-Caryophyllene
β-Ionone
Butyric acid
Pentanoic acid
-20
100
Spikes/s
B
Dsuz-ab2B
DsuzOr67a3
DsuzOr67a4
DsuzOr67a3+4
Isoamyl acetate
Pentyl acetate
Butyl acetate
Benzyl acetate
6-Methyl-5-hepten-2-ol
Isoamyl butyrate
trans-2-Hexenyl acetate
2-Heptanone
3-Methyl-1-butanol
cis-3-Hexenyl actate
3-Octanone
Citronellyl acetate
Methyl hexanoate
Butyl butyrate
α-Phellandrene
3-Nonanone
Methyl benzoate
1-Octen-3-ol
2-Nonnanone
Ethyl hexanoate
Ethyl 3-(methylthio)propionate
γ-Decalactone
Diallyl disulfide
1-Heptanol
trans,trans-2,4-Nonadienal
Ethyl-trans-2-butenoate
cis-3-Hexenyl lactate
Ethyl salicylate
Isobutyl acetate
Sabinene
Methyl octanoate
trans-2-Hexen-1-ol
Phenethyl propionate
(R)-(+)-Limonene
Hexyl-2-methylbutanoate
Ethyl benzoate
Ethyl butyrate
Methyl eugenol
cis-3-Hexenyl butyrate
(-)-Menthone
Ethyl (methylthio)acetate
Ethyl 3-hydroxybutyrate
2-Oxovaleric acid
Guaiacol
Benzyl butyrate
trans-2-Hexen-1-al
Hexanoic acid
Heptanoic acid
2-Ethylhexanoic acid
Pentanoic Acid
γ-Terpinene
Geranyl acetate
trans-2-Nonenal
2,3-Butanedione
2-methylbutyric acid
α-Terpineol
2-Phenylethylamine
β-Ionone
Farnesol
Terpinolene
2-Acetoxy-3-butanone
2-Phenylethanol
Hexyl hexanoate
Octanoic acid
Spermidine
2,3-Butanediol
4-Methyl-3-hepten-2-one
α-Ionone
Ethyl Isovalerate
4-Ethylguaiacol
2-Methyl-1-propanol
Acetophenone
p-Cresol
Ethyl-trans-2-octenoate
Butyraldehyde
1-Heptadecene
1-Nonanol
β-Cyclocitral
Ethyl dcanoate
trans-3-Hexenoic acid
Hexanal
Ammonium hydroxide
Ethyl Heptanoate
2-Methyl-1-butanol
Pyridine
Ethyl 3-hydroxyhexanoate
Acetone
3-Butenoic acid
γ-Hexalactone
(-)-trans-Caryophyllene
(S)-(-)-Limonene
Eugenol
Isobutyric acid
Valencene
β-Citronellol
farnesene
α-terpinyl acetate
(+)-Limonene oxide
Propanoic acid
Pyrrolidine
Veratrole
Diethyl succinate
4-Methylveratrole
Methyl isobutyrate
Butyric acid
Cadaverine
DEET
Ethyl octanoate
Ethyl lactate
1-Propanol
Phenylacetaldehyde
Acetic acid
Indole
α-Pinene
Isovaleric acid
1,4-Diaminobutane
Ethyl acetate
Methyl salicylate
Phenyl acetate
-50
250
Spikes/s

Figure 5

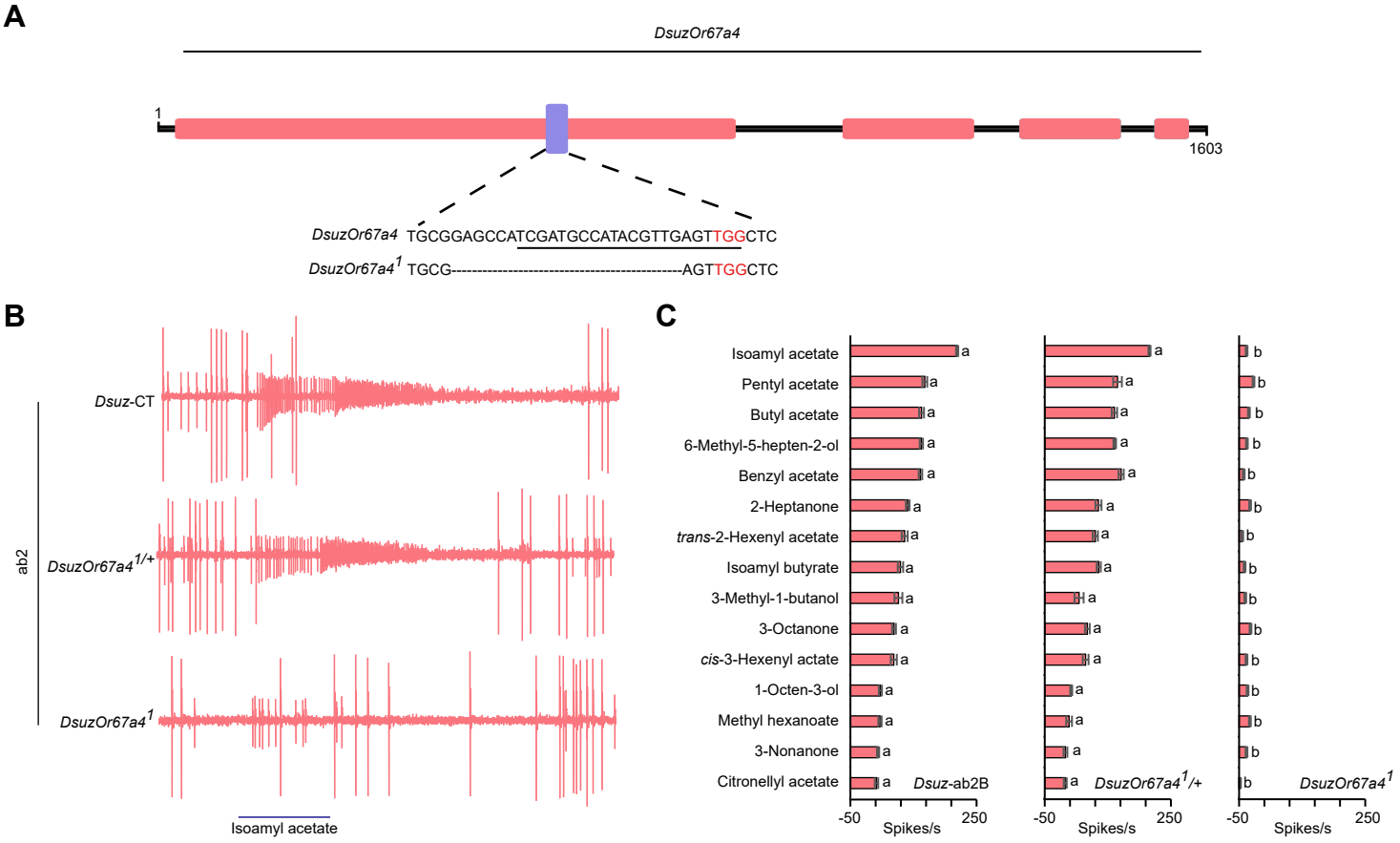
A
DsuzOr67a4
1
1603
DsuzOr67a4 TGCGGAGCCATCGATGCCATACGTTGAGTTGGCTC
DsuzOr67a4^1 TGCG----------AGTTGGCTC
B
ab2
Dsuz-CT
DsuzOr67a4^1/+
DsuzOr67a4^1
Isoamyl acetate
C
Isoamyl acetate
Pentyl acetate
Butyl acetate
6-Methyl-5-hepten-2-ol
Benzyl acetate
2-Heptanone
trans-2-Hexenyl acetate
Isoamyl butyrate
3-Methyl-1-butanol
3-Octanone
cis-3-Hexenyl actate
1-Octen-3-ol
Methyl hexanoate
3-Nonanone
Citronellyl acetate
Dsuz-ab2B
DsuzOr67a4^1/+
DsuzOr67a4^1
-50
250
Spikes/s

Figure S1

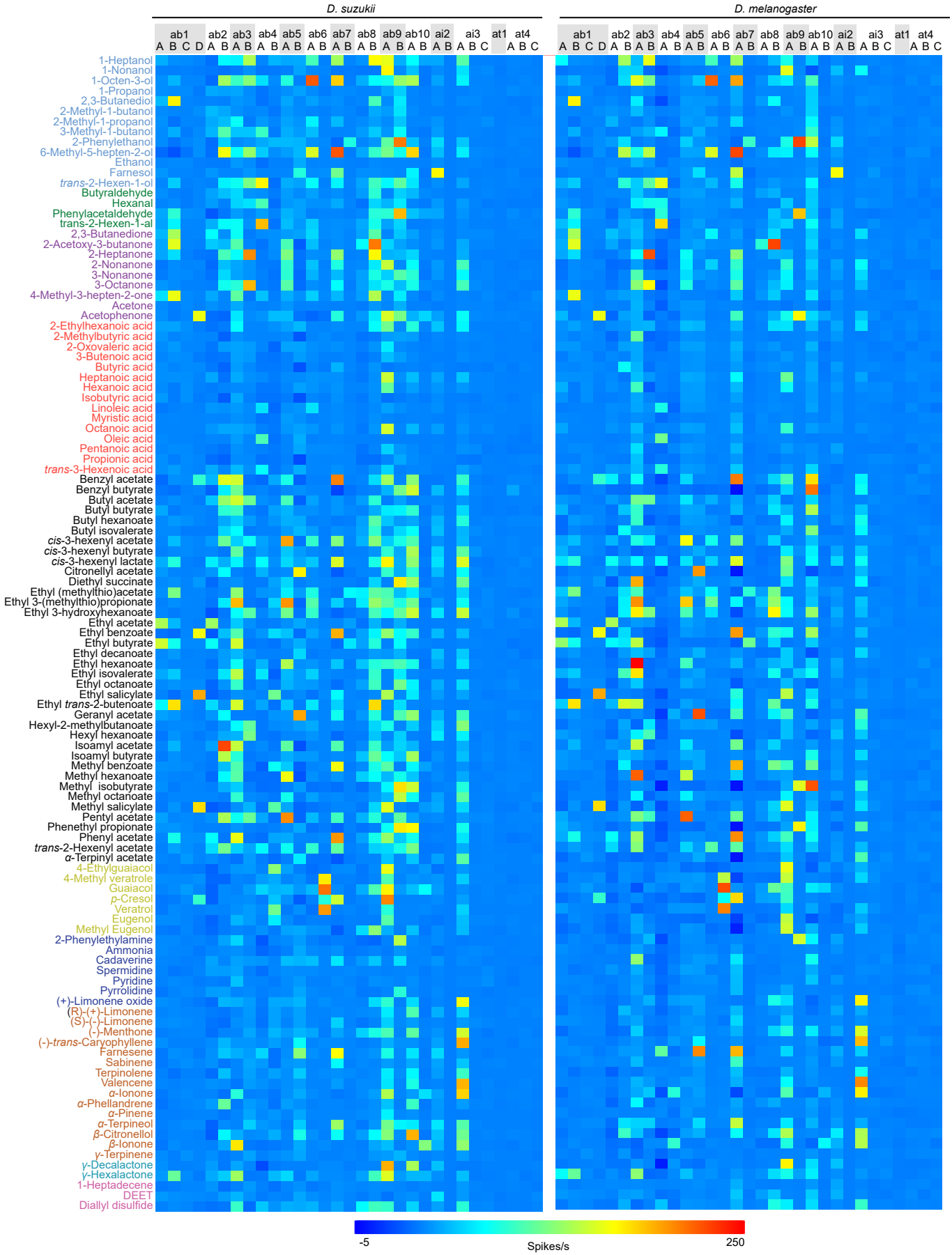
D. suzukii
D. melanogaster
ab1 A B C D
ab2 A B
ab3 A B
ab4 A B
ab5 A B
ab6 A B
ab7 A B
ab8 A B
ab9 A B
ab10 A B
ai2 A B
ai3 A B C
at1
at4 A B C
1-Heptanol
1-Nonanol
1-Octen-3-ol
1-Propanol
2,3-Butanediol
2-Methyl-1-butanol
2-Methyl-1-propanol
3-Methyl-1-butanol
2-Phenylethanol
6-Methyl-5-hepten-2-ol
Ethanol
Farnesol
trans-2-Hexen-1-ol
Butyraldehyde
Hexanal
Phenylacetaldehyde
trans-2-Hexen-1-al
2,3-Butanedione
2-Acetoxy-3-butanone
2-Heptanone
2-Nonanone
3-Nonanone
3-Octanone
4-Methyl-3-hepten-2-one
Acetone
Acetophenone
2-Ethylhexanoic acid
2-Methylbutyric acid
2-Oxovaleric acid
3-Butenoic acid
Butyric acid
Heptanoic acid
Hexanoic acid
Isobutyric acid
Linoleic acid
Myristic acid
Octanoic acid
Oleic acid
Pentanoic acid
Propionic acid
trans-3-Hexenoic acid
Benzyl acetate
Benzyl butyrate
Butyl acetate
Butyl butyrate
Butyl hexanoate
Butyl isovalerate
cis-3-hexenyl acetate
cis-3-hexenyl butyrate
cis-3-hexenyl lactate
Citronellyl acetate
Diethyl succinate
Ethyl (methylthio)acetate
Ethyl 3-(methylthio)propionate
Ethyl 3-hydroxyhexanoate
Ethyl acetate
Ethyl benzoate
Ethyl butyrate
Ethyl decanoate
Ethyl hexanoate
Ethyl isovalerate
Ethyl octanoate
Ethyl salicylate
Ethyl trans-2-butenoate
Geranyl acetate
Hexyl-2-methylbutanoate
Hexyl hexanoate
Isoamyl acetate
Isoamyl butyrate
Methyl benzoate
Methyl hexanoate
Methyl isobutyrate
Methyl octanoate
Methyl salicylate
Pentyl acetate
Phenethyl propionate
Phenyl acetate
trans-2-Hexenyl acetate
α-Terpinyl acetate
4-Ethylguaiacol
4-Methyl veratrole
Guaiacol
p-Cresol
Veratrol
Eugenol
Methyl Eugenol
2-Phenylethylamine
Ammonia
Cadaverine
Spermidine
Pyridine
Pyrrolidine
(+)-Limonene oxide
(R)-(+)-Limonene
(S)-(-)-Limonene
(-)-Menthone
(-)-trans-Caryophyllene
Farnesene
Sabinene
Terpinolene
Valencene
α-Ionone
α-Phellandrene
α-Pinene
α-Terpineol
β-Citronellol
β-Ionone
γ-Terpinene
γ-Decalactone
γ-Hexalactone
1-Heptadecene
DEET
Diallyl disulfide
-5
Spikes/s
250

Figure S2

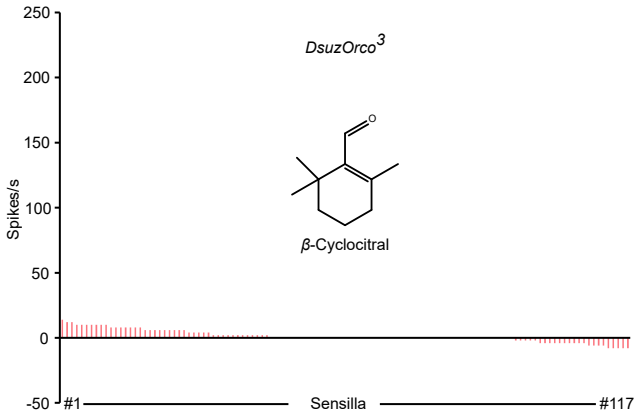
250
200
150
100
50
0
-50
Spikes/s
DsuzOrco3
O
β-Cyclocitral
#1
Sensilla
#117

Figure S3

A

```
                pid
DmelOr22a       100.0%  MLSKFFPHIKEKPLSERVKSRDAFIYLDRVMWSFGWTEPENKRWILPYKLWLAFVNIVML  60
DsuzOr22a       69.8%   MLAKFFPLIKERPLNERVQSRDAFIYLDRVMWTLGWTEPYEKRWAAVYKVFCFLTTMVCF  60
DbiaOr22a       69.0%   MLIKFFPLIKEKPLNELVQSRDAFIYLERVMWTLGWTEPYEKRWAVVYKVFSFMTSIGFF  60
                                                                          TM1
DmelOr22a       100.0%  ILLPISISIEYLHRFKTFSAGEFLSSLEIGVNMYGSSFKCAFTLIGFKKRQEAKVLLDQL  120
DsuzOr22a       69.8%   ILVPISIVVEYVRRFKSFSAGEFLSSLEIGVNMYGCSFKNTYTLLGQRKVRKAKLILDRL  120
DbiaOr22a       69.0%   ILLPLSICVEYVNRFKSFSAGEFLSSLEIGVNMCGCSFKNTYTLLGRRKVRKAKLILDRL  120
                                          TM2
DmelOr22a       100.0%  DKRCLSDKERSTVHRYVAMGNFFDILYHIFYSTFVVMNFPYFLLERRHAWRMYFPYIDSD  180
DsuzOr22a       69.8%   DERCLRDEEKSLVHRYVALGNFSYVVYHTCYWVFVITNFIGFLLIGHHAWRMFIPLLKSD  180
DbiaOr22a       69.0%   DERCLRDEEKSLVHRYVALGNFSYTVYHTCYWVFVITNFIGFLLIGHHAWRMYIPLLKSD  180
                                        TM3
DmelOr22a       100.0%  EQFYISSIAECFLMTEAIYMDLCTDVCPLISMLMARCHISLLKQRLRNLRSKPGRTEDEY  240
DsuzOr22a       69.8%   EHFLISSVAEFLLMLYVVTMAQCSDVCPTVSMLMARCHILLLQKRVLRLRSDPGKGDDED  240
DbiaOr22a       69.0%   EHFLISSVAEFLLMLYVVTMAQCSDVCPTISMLMARCHIILLRNRMMRLRSDPEKGDDED  240
                             TM4
DmelOr22a       100.0%  LEELTECIRDHRLLLDYVDALRPVFSGTIFVQFLLIGTVLGLSMINLMFFSTFWTGVATC  300
DsuzOr22a       69.8%   LEELAKCIQDHHLILDYVNTLRPVFSGVIFVQFLLIGVVLGLSMINVMFFLSFWTGLGTC  300
DbiaOr22a       69.0%   LEELTKCIQDHRLILDYVNTLRPVFSGVIFVQFLLIGVVLGLSMINVMFFLSFWTGLGTC  300
                                          TM5                            TM6
DmelOr22a       100.0%  LFMFDVSMETFPFCYLCNMIIDDCQEMSNCLFQSDWTSADRRYKSTLVYFLHNLQQPITL  360
DsuzOr22a       69.8%   LFMFDVCMETFPFCYLCNMIIDDCQDLSDSLFQSNWTSASRRYKSTLVYFLHNLQQPIIL  360
DbiaOr22a       69.0%   LFMFDVCMETFPFCYLCNIIIDDCQDLADSLFQSNWTSASRRYKSTLVYFLHNLQQPIIL  360
                                                                   TM7

DmelOr22a       100.0%  TAGGVFPISMQTNLAMVKLAFSVVTVIKQFNLAERFQ  397
DsuzOr22a       69.8%   TAGGVFPICMQTNLSMVKLAFSVVTIIKQFNLAEKFK  397
DbiaOr22a       69.0%   TAGGIFPICMQTNLSMVKLAFSVVTIIKQFNLADKFK  397
```
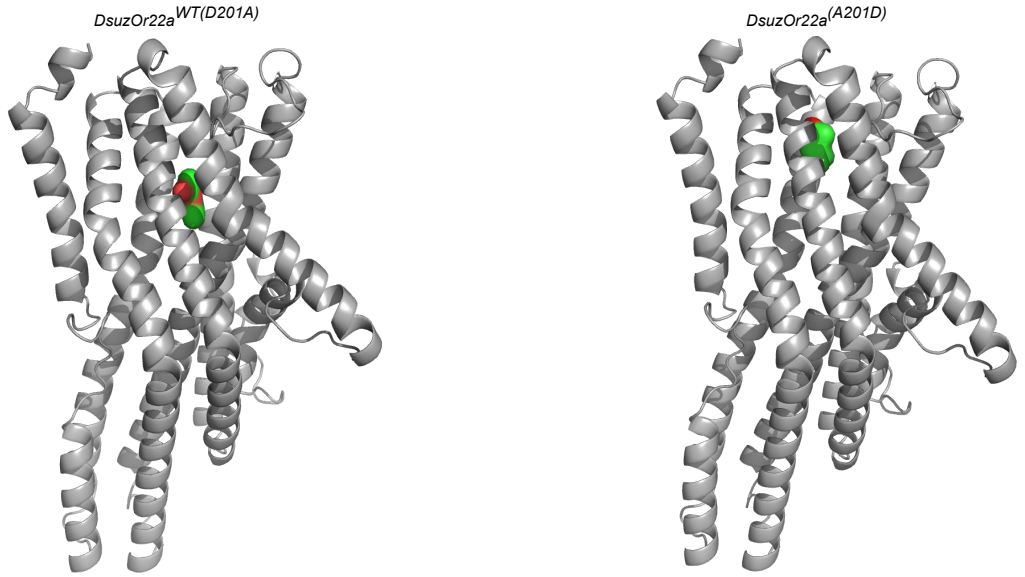
B